NASA Technical Memorandum 88881

Selection Rolling-Element Bearing Steels for Long-Life Application

Erwin V. Zaretsky
Lewis Research Center
Cleveland, Ohio

Prepared for the
International Symposium on the Effect of Steel Manufacturing Processes on the Quality of Bearing Steels
sponsored by the American Society for Testing and Materials
Phoenix, Arizona, November 4–6, 1986

NASA

SELECTION OF ROLLING-ELEMENT BEARING STEELS FOR LONG-LIFE APPLICATION

Erwin V. Zaretsky
National Aeronautics and Space Administration
Lewis Research Center
Cleveland, Ohio 44135

SUMMARY

Nearly four decades of research in bearing steel metallurgy and processing has resulted in improvements in bearing life by a factor of 100 over that obtained in the early 1940's. For critical applications such as aircraft, these improvements have resulted in longer lived, more reliable commercial aircraft engines. Material factors such as hardness, retained austenite, grain size and carbide size, number, and area can influence rolling-element fatigue life. Bearing steel processing such as double vacuum melting can have a greater effect on bearing life than material chemistry. The selection and specification of a bearing steel is dependent on the integration of all these considerations into the bearing design and application. The paper reviews rolling-element fatigue data and analysis which can enable the engineer or metallurgist to select a rolling-element bearing steel for critical applications where long life is required.

E-3288

INTRODUCTION

Through the use of improved technology, rolling-element bearing life and reliability has increased dramatically over the last four decades. A chart showing the major advances contributing to these life improvements is shown in Fig. 1 [1]. The major reason for these advances has been the rapidly increasing requirements of aircraft jet engines from the early 1950's to the present.

Starting in the early 1940's, new developments in the making of bearing steels began. The improved steel-making developments were primarily initiated by the acceptance of a comprehensive material specification for AMS 6440 and AISI 52100 steel (A, Fig. 1). New heat-treatment equipment became available in 1941 which incorporated improved temperature controls and recorders. The use of neutral atmospheres during heat treatment eliminated, for all practical purposes, surface decarburization (B, Fig. 1).

As the requirement for bearing steel increased, large electric arc furnaces were installed which produced larger size billets. These larger billets necessitated working the material to reduce the billets to size for tubing or individual forgings. The working of the bearing steel refines the steel grain and carbide size and reduces the size of the materials inclusions and segregates (C, Fig. 1). This trend toward larger furnace size has continued to this time [1].

Major advances in melting practice evolved over a period covering 1952 to the early 1970's. Immersion thermocouples were introduced in 1952 (D, Fig. 1). These thermocouples permitted better control of steel melting [1].

Some significant manufacturing process changes were made in the 1950's. Shoegrinding (E, Fig. 1) was introduced about 1953. This method improved race surface quality and tolerance. With this grinding method, it is practically

impossible to grind eccentricity and face runout into the bearing race. Also, the transverse radii of the races, controlled by the grinding wheel dresser, are more consistent [1].

The vacuum degassing and vacuum melting processes were introduced to the bearing industry in the late 1950's. Consumable-electrode vacuum melting was one such process (F, Fig. 1). Vacuum melting releases entrapped gasses and reduces the quantity and alters the type of inclusions and trace elements present in the steel.

In order to assure clean steel with the vacuum-melting processes, nondestructive testing, using eddy current and ultrasonic methods, was applied to billets, bars, and tubing (G, Fig. 1). This assured the quality of the steel for the bearing manufacturing process.

In rolling-element bearings the elastically deformed rolling-element surfaces are separated by a thin lubricant film referred to as an elastohydrodynamic film [2]. The concept of elastohydrodynamic (EHD) lubrication while recognized in 1949 [3] was further recognized as a significant factor in affecting bearing fatigue life and wear (H, Fig. 1). By controlling the EHD film thickness through lubricant selection and control of operating conditions together with the improvements in surface finish, rolling-element bearings were able to operate at higher temperatures and for longer times [4].

In the 1960's, argon atmosphere protection of the molten steel during teeming was introduced (I, Fig. 1). Drastic improvement in micro- and macroscopic homogeneity and cleanliness with a resultant improvement in fatigue was realized [1].

Prior to the 1950's as-ground races were hand polished to improve finish and appearance. Overly-aggressive polishing could create a thin layer of plastically displaced or smeared material which was softer and more prone to fatigue failure. This manual process was replaced by mechanized honing in which all parts are smoothed in a more uniform manner (J, Fig. 1).

In 1958, NASA published their results of controlled fiber or grain on the effect of bearing life [5,6]. Controlled fiber can be obtained by forging to shape the raceway of angular-contact ball bearings. Forged raceways with controlled fiber orientation was introduced in 1963 (I, Fig. 1). This innovation improved the life of angular-contact ball bearings.

Work performed by NASA beginning in the late 1950's on material hardness effects culminated with the discovery of the differential hardness principle or controlled hardness (J, Fig. 1) [7]. Prior to this time, significant variations between rolling-element and race hardnesses could result in significant reduction in bearing life.

Combining improved surface finishes obtained by honing, improved lubricants whose selection was based upon elastohydrodynamic principles, controlled fiber and hardness, consumable-electrode vacuum melted (CEVM) AISI M-50 steel, as well as improved nondestructive inspection of the steel billet, relative bearing life of approximately 13 times the 1940 standard was achieved in 1975 [4]. The NASA research culminated by using, for the first time, vacuum-induction melted, vacuum-arc remelted (VIM-VAR) AISI M-50 (K, Fig. 1) demonstrating lives in excess of 100 times the 1940 standard at speeds to three million DN [8]. The improvement in lives with the VIM-VAR process was accompanied by improved product consistency by reducing human element variability through better process controls and audits (L, Fig. 1) [1].

In 1983, Bamberger [9] at the General Electric Co. developed a significantly improved AISI M-50 steel which he called M-50NiL which was capable of being case hardened and exhibited lives in excess of through hardened VIM-VAR AISI M-50 (M, Fig. 1).

The steel technology for long-life bearing application has, over the last 20 years, reached a 20-fold increase in life potential. The object of this paper is to review rolling-element fatigue data and analysis which can enable the engineer or metallurgist to select and specify a rolling-element bearing steel for critical application where long life is required.

MATERIAL CLEANLINESS

Rolling-element fatigue is a mode of failure that occurs in rolling-element bearings such as ball and roller bearings. It is a cyclic-dependent phenomenon resulting from repeated stresses under rolling-contact conditions. Fatigue can be affected by many variables, such as rolling speed, load, material, sliding within the contact zone, temperature, contact geometry, type of lubricant, and others. The fatigue failure manifests itself initially as a pit which, in general, is limited in depth to the zone of resolved maximum shearing stresses and in diameter to the width of the contact area (Fig. 2).

Research performed by Bear, Butler, Carter, and Anderson [5,6,10] substantiated the early findings of Jones [11] that one mode of rolling-element fatigue is due to nonmetallic inclusions. These inclusions act as stress raisers similar to notches in tension and compression specimens or in rotating beam specimens. Incipient cracks emanate from these inclusions, enlarge and propagate under repeated stresses forming a network of cracks which form into a fatigue spall or pit. In general the cracks propagate below the rolling-contact surface approximately 45° to the normal;

i.e., they appear to be in the plane of maximum shearing stress (Fig. 3). Carter [10] made a qualitative generalization that the location of an inclusion with respect to the maximum shearing stress is of prime importance. Based on observations of inclusions in SAE 52100 and AISI M-1 steels, Carter concluded that:

(1) Inclusion location is of primary importance

(2) Size and orientation are also important

(3) The oxides and larger carbides are more harmful than the softer sulfide inclusions, and

(4) Inclusions, carbides, and irregular matrix conditions appear slightly less harmful to fatigue life in SAE 52100 than in AISI M-1.

Carter's conclusions were substantiated by Johnson and Sewell [12]. The results of their work are summarized in Fig. 4. They show that as the total number of alumina and silicates increase, fatigue life decreases. However, they indicate that the increase in sulfides may have a positive effect upon fatigue life. In addition to inclusions, material defects such as microcracks, trace elements, or unusual carbide formations present in the material can contribute to failure. An attempt was made by NASA in the early 1960's to manufacture 12.7 mm (0.5 in.) diameter AISI 52100 steel balls with increased sulfur content. This effort resulted in balls having incipient cracks in their matrices.

One method for increasing rolling-element reliability and load capacity is to eliminate or reduce nonmetallic inclusions, entrapped gases, and trace elements. Improvements in steel-making processing, namely melting in a vacuum, can achieve this. These vacuum-melting techniques include vacuum induction melting (VIM) and consumable-electrode vacuum melting (CVM) or vacuum-arc melting (VAR) as well as vacuum degassing.

It is possible with any of these melt techniques to produce material with a lower inclusion content than air-melted material, particularly those inclusions which are generally considered to be more injurious, such as oxides, silicates, and aluminates. These inclusions are, in part, the result of standard air melt deoxidation practice which involves the use of silicon and aluminum. Exposing the melt to a vacuum permits deoxidation to be performed effectively by the carbon. The products formed when using carbon as a deoxidizer are gaseous, and thus are drawn off in the vacuum. Further, these techniques permit extremely close control of chemistry and also permit production of variations in chemical analysis which was at one time impractical.

Fatigue tests of 6309-size deep-groove ball bearings made from two heats of AISI M-50 steel produced by the consumable-electrode vacuum-melting (CVM) process resulted in an average 10-percent life (L_{10}) of 4.2 times the catalog life of 10 million revolutions. Additional fatigue tests of the same type of bearings made from a single heat of air melted AISI M-50 steel resulted in a life of only 0.4 times the catalog rating [13].

The improvement in life of bearings made of vacuum-melted steels does not appear to be commensurate with the improvement in cleanliness. This, of course, upholds the long-held theory that cleanliness is not the only factor involved in bearing fatigue. Even in exceptionally clean materials, nonmetallics are present to some degree and, depending on the magnitude and location in relation to the contact stresses, can be the nucleus of fatigue cracks as previously discussed. A single heat of primary air melted AISI 52100 steel was processed through five successive consumable-electrode vacuum remelting cycles. Groups of 6309-size bearing inner-races were machined from material taken from the air-melt ingot and the first, second, and fifth remelt

ingots for evaluation; they were then heat treated and manufactured as a single lot to avoid group variables. With each remelt, a progressive reduction of nonmetallic content occurred. Endurance results, summarized in Fig. 5, show that the L_{10} life appears to increase for successive remelting with the fifth remelt material reaching a life approximately four times that of the air melt group [14].

Based upon the above, it becomes apparent that significant increases in rolling-element fatigue life and, thus, bearing life and reliability can be achieved through the use of successive remelting of the bearing steel. Recognizing this fact, Bamberger, Zaretsky, and Signer [8] had 120-mm bore angular-contact ball bearings manufactured from a single heat of vacuum-induction melted, vacuum-arc remelted (VIM-VAR) AISI M-50 steel. This was perhaps the first time this double vacuum melting process was used for aircraft quality bearings. Two groups, each comprising thirty of these bearings, were endurance tested at a speed of 12 000 and 25 000 rpm (1.44×10^6 and 3.0×10^6 DN, where DN is a speed parameter determined by multiplying the bearing bore in millimeters by the bearing speed in rpm), respectively. Test conditions for these tests are given in Table 1. At 1.44×10^6 and 3.0×10^6 DN, 84 483 and 74 800 bearing test hours were accumulated, respectively. The results of these tests are shown in Fig. 6 and summarized in Table 1. Bearing lives at speeds of 3×10^6 DN with the VIM-VAR AISI M-50 were nearly equivalent to those obtained at lower speeds. These test results were compared with similar bearings made from CVM AISI M-50 steel run under the same conditions. At 3.0×10^6 DN, the life was in excess of 44 times that predicted on the basis of air-melt steel, approximately 23 times that using CVM steel [15] and 7.6 times that using the ASME life adjustment factors [16] based upon CVM AISI M-50 steel (see Fig. 6). Further work

performed at the General Electric Co. [17] using the rolling-contact (RC) tester which compared air melted and vacuum arc remelted (AM-VAR), double vacuum arc remelted (VAR-VAR), and VIM-VAR AISI M-50. The results of these tests are shown in Fig. 7. The VIM-VAR material produced average 10-percent lives 1.9 and 1.5 those of the AM-VAR and VAR-VAR materials, respectively. These tests which are run at 4.83×10^9 N/m^2 (700 000 psi) and others of a similar nature tend to compress life differences because of the high Hertz stress at which they are run. However, rolling-element fatigue tests run in the NASA five-ball fatigue tester at 5.52×10^9 N/m^2 (800 000 psi) with 12.5 mm (0.500 in.) diameter balls made from VIM-VAR AMS 5749 and VIM AMS 5749 resulted in the VIM-VAR material have a life 14 times the VIM AMS 5749 [18].

Even with the best quality assurance in steel melting, it is always possible for large inclusions or segregates to be encased within the billet or in the final end product. Nondestructive testing of the billet or bearing is a final step to assure the life and reliability of the end product. The most successful use of ultrasonics as an inspection tool was reported by Koved and Rospond [19]. Roller bearings made of AISI 8620 were arranged into three groups based on differences in the size and the frequency of ultrasonic indications. The individual bearings were rated by a method that assigned a numerical value to their ultrasonic pattern. The number was based on the frequency of indications and included a weighting factor for size. These numerical ratings were subsequently converted into qualitative ratings.

The fatigue life distributions for the ultrasonically-rated groups of bearings are shown in Fig. 8. The three performance curves separate nicely in the same order as their ultrasonic classification. The group characterized as ultrasonically poor demonstrated the worst performance, average quality was intermediate, and good quality clearly exhibited the best fatigue-life

distribution. Thus, ultrasonic inspection has the capability of differentiating, on a statistical or group basis, relative material quality in terms of life performance.

MATERIAL HARDNESS

Heat treatment can significantly influence several rolling-element bearing material properties. Most bearing procurement specifications do not designate heat treatment but rather call for certain material characteristics such as grain size and hardness, which are controlled by the heat treat cycle. Hardness is the most influential heat treat induced variable in rolling-element fatigue [20,21]. In general, the higher the material hardness the longer the life. A relationship was introduced by Zaretsky [4] based upon the work reported in [7] which approximates the effect of bearing material hardness on fatigue life.

$$\frac{L_2}{L_1} = e^{m(R_{c2} - R_{c1})} \tag{1}$$

where L_1 and L_2 are the bearing 10-percent lives at bearing hardnesses of R_{c2} and R_{c1}, respectively, and m is a material constant which can be taken as 0.1. It is assumed for the purpose of this relationship which was obtained for AISI 52100 that all components in the rolling-element bearing, that is, the rolling elements and races, are of the same hardness. It was further assumed that this equation can be extended to other bearing steels.

In the 1960's, it was assumed by the bearing industry that materials which had higher amounts of alloying elements would have a better hardness retention at elevated temperature. It was reasoned that this would also result in a higher ambient temperature hardness as well as longer bearing life. However, no systematic study was performed and published which would

confirm these assumptions. Beginning in the early 1970's such a study was undertaken at NASA [23-25]. The results of this study were most revealing, completely changing those assumptions previously held.

Short term hot hardness measurements were made for groups of through hardened specimens of AISI 52100, AISI M-1, AISI M-50, Halmo, WB-49, AISI 440C, WD-65 and Matrix II. Measurements were also made of case-hardened specimens of Super Nitralloy (5Ni-2Al), AISI 8620, CBS 600, CBS 1000, and Vasco X-2. The results for the through hardened materials and for the case hardened materials were normalized and are shown in Figs. 9 and 10, respectively. These normalized data show that regardless of the initial hardness, the hot hardness of the individual materials shows the same functional dependence. That is, the changes in hardness with increasing temperature are independent of material composition or room temperature hardness.

The data of Figs. 9 and 10, when plotted on log-log coordinates [23], can be represented by a straight line having the form

$$(Rc)_T = (Rc)_{RT} - \alpha \Delta T^{\beta} \qquad (2)$$

where

$(Rc)_T$ Rockwell C hardness at operating temperature

$(Rc)_{RT}$ Rockwell C hardness at room temperature

ΔT change in temperature, $T_T - T_{RT}$, K, (°F)

T_T operating temperature, K (°F)

α temperature proportionality factor, $K^{-\beta}$ ($°F^{-\beta}$)

β exponent

Values for α and β for various materials are given in Table 2.

From equation (1), let L_1 be the bearing life calculated according to [26]. Hence,

$$L_1 = \left(\frac{C}{P}\right)^n \tag{3}$$

where C is the basic dynamic load rating of the bearing and P is the equivalent load [26]. Assume, based upon experience, that the basic load rating is based upon a material hardness of Rockwell C60. As a result, Eq. (1) can be written

$$L_2 = e^{m[(Rc)_T - 60]}\left(\frac{C}{P}\right)^n \tag{4}$$

Combining Eqs. (2) and

$$L_2 = e^{m\{[(Rc)_{RT} - 60] - \alpha(T_T - T_{RT})\}^{\beta}}\left(\frac{C}{P}\right)^n \tag{5}$$

where T_{RT} equals 294 K (70 °F).

From the above equation, the life of a rolling-element system can be determined as a function of room temperature hardness and operating temperature for a particular steel.

Long-term hot-hardness studies were performed with five vacuum-melted steels tempered to various room-temperature hardnesses: AISI 52100 and the tool steels AISI M-1, AISI M-50, Halmo, and WB-49 [27]. Hardness measurements were taken at both room temperature and the soak temperature at regular intervals until 1000 hr of soak time were accumulated. AISI 52100 was tested at temperatures to 478 K (400 °F), and the other bearing steels were tested at temperatures to 700 K (800 °F). With the exception of the AISI 52100, none of the steels tempered (permanently lost hardness) during soaking. The AISI 52100 steel that was initially hardened to Rockwell C 62.5 or 64.5 lost hardness during the first 500 hr of the 1000-hr soak tests at temperatures greater than 394 K (250 °F), but it maintained its hardness during the final

500 hours of soaking. Similarly, AISI 52100 that was initially hardened to Rockwell C 60.5 lost hardness during the first 500 hr of the 1000-hr soaking at temperatures greater than 422 K (300 °F), but it maintained its hardness during the final 500 hr of soaking. The results of these tests for AISI 52100 are summarized on Table 3. Like and similar results may be expected for other lower tempering temperature-bearing steels.

The effect of component hardness combinations on the fatigue life of AISI 52100 rolling elements subjected to repeated stresses applied in rolling contact was studied in the NASA five-ball fatigue tester [7,28]. Groups of upper test balls (analogous to the inner race of a bearing) with nominal Rockwell C hardnesses of 60, 63, and 65 were run against lower test balls (analogous to the balls of a bearing) of nominal Rockwell C hardnesses of 60, 62, 63, 65, and 66. These results indicated that, for a specific upper test ball (race) hardness, the rolling-element fatigue life and load-carrying capacity of the test system increased with increasing lower test ball hardness to an intermediate hardness value where a peak life was attained. The peak life-hardness combination occurred for each of the three lots of upper test balls (races) in which the hardness of the lower test balls was approximately 1 to 2 points Rockwell C greater than that of the upper test ball (race). According to these results, for AISI 52100 steel, a maximum bearing fatigue life should occur when the balls of the bearing are 1 to 2 points harder than the races.

Rolling-element fatigue tests were then performed on AISI 52100 207-size deep-groove ball bearings with inner and outer races from the same heat of air melt material tempered to nominal Rockwell C hardnesses of 63 and balls from a second heat of air-melt material tempered to nominal Rockwell C hardnesses of 60, 63, 65, and 66 [28,29]. Subsequent to testing, the bearings were

regrouped according to their actual values of ΔH for Rockwell C hardness increments of 0.5 and 1.0, where ΔH is the difference between the actual hardness of the rolling elements in the bearing and the actual hardness of the inner race. The results of these tests are shown in Fig. 11. Other bearing data taken from [30] were reanalyzed and plotted in Fig. 12. Both sets of bearing data exhibited a maximum life at a ΔH of approximately 1 to 2 points Rockwell C. These results correlated with those obtained with the five-ball fatigue tester.

The research of [7,28] was repeated by Zaretsky for CVM AISI M-50 steel. The results of this research are unpublished. In general, the AISI M-50 results produced increasing life with increasing hardness and ΔH to values of ΔH equal zero. At values beyond zero, life remained unchanged in contrast to the results of the AISI 52100 material where life peaked at ΔH values of 1 to 2 points Rockwell C and then began to decrease. Based upon these tests, it may be reasonably concluded that, for elevated temperature operation, care should be taken to match the hardnesses of the rolling elements and the raceways while maintaining the highest material hardness for all components.

CARBIDE EFFECTS

From the data of [31-33] summarized in Table 4, it was speculated that an interrelation existed among median residual carbide size, number of residual carbide particles per unit area and the percent area of residual carbides and rolling-element fatigue life. Residual carbides are those carbides that do not go completely into solution during austenitizing and are a function of the alloying elements and heat treatment. This is opposed to the hardening carbide precipitates, which precipitate upon aging at the tempering temperature. The carbides referred to in the following will be the residual carbides.

If the carbides in a material are the nucleation site of an incipient fatigue failure, then the probability of survival S for a lot of specimens or a single specimen can be expressed as a function of three variables (1) percent area of carbides, a, (2) median carbide size (length), m, and (3) total number of carbides per unit area, n [34, 35]. Based upon a statistical analysis a carbide factor C' can be derived where

$$C' = \frac{L_3}{L_2} \tag{6}$$

In [31-33] AISI 52100 is the material which produced the highest life values. Therefore, the values for the carbide factor C' can be normalized with respect to the AISI 52100 material. Thus,

$$C' = \frac{1}{K_1\left(\frac{m}{0.26} + \frac{718}{n} + \frac{\alpha}{9.54} + \frac{K_4}{K_1}\,Co\right)} \tag{7}$$

From experimental data, K_1 and K_4 were empirically determined to be 1/3 and 4/3, respectively [34,35] and Co is the weight percent of cobalt in the material.

Table 4 summarizes the carbide factors for the data of [31-33]. In Fig. 13 the relative material L_{10} lives are plotted against the carbide factor C'. There appears to be a reasonable correlation between the carbide factor C' and relative life. For the individual groups of data and the combined groups the confidence number was found to be 0.87 and 0.83, respectively. This means that the carbide factor C' can give a reasonable prediction of relative life under identical conditions of material hardness and lubrication mode. Thus, the carbide parameter seems to transcend such variables as heat treatment, chemical composition, and hardening mechanism to predict the lives of individual lots. The carbide parameter may also be applicable to conventional fatigue (i.e., bending, rotating-bending, etc.).

Research reported in [36] for AMS 5749 material further substantiated the negative effect of large carbide size and banded carbide distribution on rolling-element fatigue life. Endurance tests were run with ten 46-mm bore split-inner ring angular-contact ball bearings made from VIM-VAR AMS 5749 steel. The inner and outer rings were machined from bars. No forging process was used. Test conditions included a thrust load of 4890 N (1100 lb) at a speed of 42 000 rpm and an oil in temperature of 366 K (200 °F). The resultant 10-percent fatigue life of the bearings was 32 hr as compared with a predicted life of 1900 hr, a reduction in life of 98 percent.

Metallurgical examination of the raceways revealed large size carbides and severe banding of the carbides in the raceways. Also, the carbide stringers or grain flow were oriented at an angle to the contact surfaces, since the bearings were run with a thrust load and the balls run at an angle to the bearing axis. The early failures in these bearings were attributed to the undesirable carbide structure and, in particular, the large carbide stringers that were at or very near the rolling surface [36]. Hence, while previous testing [18] had shown AMS 5749 steel to have rolling-element fatigue lives at least equivalent to VIM-VAR ASIS M-50, the presence or orientation of the carbides severely reduced the bearing life [36].

There appear to be two distinct criteria in the selection of a through-hardened rolling-element bearing steel. First, rolling-element fatigue life is a function of material hardness. Second, life is a function of carbide size, area, and number as represented by the carbide factor. These two criteria can be combined to both determine and evaluate without extensive testing the fatigue life of a bearing material or groups of materials. Combining Eqs. (5), (6), and (7), dropping the subscripts 2 and 3, and

letting $L_A = L_3$ where L_A is the expected bearing life at a 90-percent probability of survival

$$L_A = kC'e^{m\{[(Rc)_{RT} - 60] - \alpha(T_T - T_{RT})^{\beta}\}}\left(\frac{C}{P}\right)^n \tag{8}$$

where k is a factor which combines processing and environmental factors which can affect bearing life [35]. The values of m can reasonably be assumed to be equal to 0.1. Values for α and β can be obtained from Table 2. For ball and roller bearings n is equal to 3 and 10/3, respectively.

A method to reduce the size of the carbides in a material is called ausforming [37]. The ausforming process consists of an isothermal "warm working" operation performed while the material is in a metastable austenitic condition. The austinite is subsequently transformed in either the lower banite or the martensite transformation region of the time-temperature-transformation (TTT) curve. If the ausforming method is to be applied, the steel must have a sluggish transformation behavior in the temperature range where "warm working" is to take place. AISI M-50 is such a steel [37].

Initial rolling-element fatigue tests were performed with cylindrical rollers made from ausformed AISI M-50 material having 40, 70, and 80 percent deformation [37]. The results of these tests are shown in Fig. 14. It can be seen that the ausformed material is superior to the normally processed AISI M-50. Additionally, a relation exists between the amount of deformation during ausforming and fatigue life. Tests with ausformed AISI M-50, 35-mm bore, single-row radial ball bearings [38] having 80-percent deformation produced fatigue lives approximately eight times conventionally forged AISI M-50 bearings.

Ausformed balls were fabricated from AISI M-50 bar material which was extruded to a cross-sectional area 20 percent of the original area (80-percent reduction in cross-sectional area) while the material was in a metastable austenitic condition. The 10-percent fatigue life of this group of ausformed balls was three and four times that of two groups of conventionally processed AISI M-50 balls [39].

It is believed that the primary mechanism causing the improved fatigue life is "strain induced precipitation." In essence, sufficient energy is imparted to the material during ausforming which results in precipitation of the carbides in the material. This results in smaller and more uniformly dispersed carbides because of the availability of a larger amount of carbide nucleation sites during the ausforming process [37].

Unpublished data from NASA tests performed with VIM-VAR AISI M-50 120-mm-bore angular-contact ball bearings made by ausforming showed that forging laps were induced in the raceways of the bearing because of the relatively low forging temperature. These forging laps acted as nuclei for fatigue spalls in a rather short period of time. The conclusion reached is that ausforming can result in improved rolling-element fatigue life, but problems with forging, particularly the large, massive parts and the costs thereof, far exceeded its benefits.

CONTROLLED FIBER

A technique which has been used to improve bearing life is the manipulation of the material fiber orientation. The races and rolling elements of most bearings are forged. Any metallic object formed by forging generally possesses a fiber-flow pattern which reflects the flow of metal during the forging operation. Carbides and nonmetallic inclusions are progressively and directionally oriented during each forming operation from

the ingot to the final bearing-element shape. Although the desired microstructure is obtained by heat treatment, the carbides and inclusions generally retain their processing-induced directionality. This pattern is fibrous in appearance when the part is macro-etched, hence the term "fiber-flow lines." In addition, the entire grain pattern is preferentially oriented in the same manner.

The type of forging used to produce rolling-element bearing components will determine the fiber pattern which exists in these bearing parts. Steel balls are usually fabricated by upsetting between hemispherical dies. This fabrication technique produces a fiber-flow pattern with two diametrically opposed areas having fibers oriented approximately perpendicular to the surface as illustrated in Fig. 15. These areas are commonly known as the poles. The excess metal extruded from between the two dies produces a thin band of perpendicularly oriented fiber when the flashing at the die parting line is removed. This line, when present, is commonly termed the "equator." Thus, a typical ball has several surface areas with varying fiber-orientation. The initial effect of fiber orientation on fatigue life was reported in [5,6]. Two lots of AISI 52100 balls were modified during manufacture to predetermine the axis of rotation and to enable one lot to be run over the poles and the other lot over the equator. The results obtained indicated a significant improvement in fatigue life when the test track passed over areas other than the poles.

Fatigue data obtained with ten different ball materials was also examined with respect to the location of specific spalls on the ball test specimens. Each of the ball specimens was destructively etched after the test to indicate the location of the failure relative to the pole areas. These data showed

that a small increase in failure density occurs at the equator where the thin band of perpendicular fiber exists and that a very significant increase in failure density occurred in the polar areas or regions where fiber is essentially perpendicular to the test surface.

Attempts were made to control fiber flow in balls [40], but these were either unsuccessful or did not produce any significant improvement in fatigue life.

While the feasibility of controlling fiber flow in balls is questionable, the opposite appears to be true in bearing races. Additional research [10] with controlled fiber flow was performed by machining race cylinders from a billet of AISI T-1 steel at various angles to the direction of forging as illustrated in Fig. 16. Three cylinders (races) were machined with axes parallel to, at 45° to, and perpendicular to the direction of fiber flow. The first cylinder (race) had fiber flow parallel to the test surface, the second had fiber orientation ranging continuously from parallel to 45° to the test surface, and the third had fiber orientation ranging continuously from parallel to perpendicular to the test surface. The 0° cylinder (race) had the best life while the 0° to 45° and the 0° to 90° cylinder (race) indicated that five of the six lowest lived failures occurred in the 81° to 90° zone. The 10-percent life for perpendicular fiber was found to be about 1.25 million stress cycles as compared with 4.7 million stress cycles for parallel fiber.

Experiments confirming the results of [5,6] were reported in [41]. Bearings were manufactured by two methods [41] as shown in Figs. 17 and 18. One method produced races with conventional fiber orientation (Fig. 15). The other method incorporated forging techniques which produced parallel fiber flow (Fig. 18). Fatigue results from these two methods show at least a ten-fold increase in life of the bearings having side grain or fiber flow

parallel to the race as opposed to bearings made with the end grain races or fiber nearly perpendicular to the running track. It was also determined that the same heats of steel which gave poor life when forged with end grain in the race performed very creditably when forged with side grain in the race. The life of parts seemed less sensitive to steel quality variations when forged with the fiber flow parallel to the race.

If bearings with side grain (parallel fiber flow) were radially loaded, no difference in life would be expected between these bearings and those conventionally forged. The reason for these results is that the conventionally forged bearing will generally produce parallel fiber flow in the portion of the race groove which is subject to the radial load. However, where the material is laden with large carbides, at or near the surface, the effect of fiber orientation or orientation of the carbide bands will have an insignificant effect on rolling-element fatigue life [36].

RESIDUAL STRESSES

An analysis presented in [42] indicates that a compressive residual stress that exists at the depth of the maximum shearing stress can decrease the maximum shearing stress. A similar analysis for superimposed stresses was subsequently reported in [43,44]. Although observations [45] would indicate that the maximum orthogonal shearing stress is the critical stress in the initiation of fatigue cracks, there also is evidence [10,11,46,47] that the maximum shearing stress is the most significant stress in the fatigue process. Thus, if the maximum shearing stress for a given Hertz stress could be decreased by compressive residual stresses, rolling-element fatigue life could be increased [42].

Residual stress can either increase or decrease the maximum shearing stress according to the following equation:

$$(\tau_{max})_r = -\tau_{max} - \frac{1}{2}(\pm S_r) \tag{9}$$

where τ_{max} is the maximum shearing stress, $(\tau_{max})_r$ is the maximum shearing stress modified by the residual stress, and S_r is the residual stress, the positive or negative sign indicating a tensile or compressive residual stress, respectively [42]. Accordingly, a compressive residual stress would reduce the maximum shearing stress and increase fatigue life according to the inverse relation of life and stress to the 9th power where

$$L \propto \left[\frac{1}{(t_{max})_r}\right]^9 \tag{10}$$

Compressive residual stresses induced beneath the surface of ball-bearing race grooves were found beneficial to rolling-element fatigue life [48,49]. Ball bearing lives were increased by a factor of 2 when metallurgically induced ("prenitrided") compressive residual stress was present in the inner rings (group B, Fig. 19) [48]. Compressive residual stresses induced by unidentified "mechanical processing" operations were also found to be beneficial to the fatigue life of ball bearings [49].

Koistinen [50] reported a method of producing compressive residual stresses in the surface of AISI 52100 steel by austenitizing in an atmosphere containing ammonia. Stickels and Janotik [51] also induced compressive residual stress in the surfaces of AISI 52100 steel rolling-element specimens by austenitizing them in a carburizing atmosphere, even though the austenitizing temperature was below that needed to dissolve all primary carbides. The depth of the compressed residual surface stress was 0.3 mm

(0.012 in.) having a maximum compressive residual stress of 0.6 N/m^2 (87 ksi). The carburized case (surface layer) contained a larger volume fraction of primary carbides, more retained austenite and was slightly harder than the core. Rolling-element fatigue tests in the RC fatigue tester at a maximum Hertz stress of 5.03×10^9 N/m^2 (729 ksi) having a depth to the maximum shearing stress of 0.015 mm (0.006 in.) resulted in the AISI 52100 which was treated in the carburizing atmosphere having a life approximately 1-1/2 times greater than the untreated AISI 52100 [52]. This increase in life can be attributed to the induced residual stresses in the region of resolved maximum shearing stresses in spite of the increased presence of carbides at or near the surface. From [52] it is apparent that the distribution of the induced compressive residual stresses is a fraction of the carbon potential. For ball and roller bearings the zone of maximum resolved shearing stresses due to Hertzian loading occur at a depth from 0.10 to 0.25 mm (0.004 to 0.010 in.) below the surface. With a carbon potential of 0.9 wt % carbon in iron, effective compressive residual stresses were available to a depth of 0.3 mm (0.012 in.). This depth was sufficient to have a beneficial effect. For the carbon potentials less than 0.7 wt % carbon high, tensile residual stresses were present at depths to 0.2 mm (0.008 in.). Hence, without taking due care, it is also possible to reduce the fatigue life potential using the carburizing process to induce residual stresses.

Compressive residual stresses can be induced as a result of the cyclic concentrated contact in rolling-element bearings [46,53-56]. These stresses depend on plastic deformation of the microstructure. They tend to reach a maximum at a depth of several mils beneath the rolling surface corresponding approximately to either the depth of the maximum shearing stress [43,55,56] or the depth of the maximum orthogonal shearing stress [46]. The magnitude of

the residual stress tangential to the surface in the direction of rolling is dependent on both the applied load and the number of load cycles. Research reported in [53] indicated a threshold load below which significant residual stresses are not induced except for very long running times.

Changes in microstructure (phase transformations) have been reported to occur in the same areas as the maximum induced residual stress [53,55]. Under some conditions of very high contract stresses, no microstructural alteration was apparent where significant residual stresses were induced in a few cycles [53]. The correlation of induced residual stress with these microstructural alterations is not clear. In [56], they are proposed to be independent phenomena. However, it is probable that some or all of the induced residual stress may be attributed to the transformation of retained austenite to martensite.

It was reported in [46] that there were significant effects of residual stress induced during fatigue testing on rolling-element fatigue life. In this work, maximum compressive residual stresses were induced and maximum fatigue life resulted when the ball hardness was 1 to 2 points Rockwell C greater than the race hardness (ΔH = 1 to 2 points Rockwell C). An identical effect is reported in [56].

It was hypothesized that such a beneficial compressive residual stress could be induced by prestressing a ball-bearing inner race; for example, by running the bearing at a load greater than the threshold load [53] for a prescribed number of cycles. The bearing, when subsequently run under more nominal service loads, would then be expected to experience a longer fatigue life.

In order to confirm the above hypothesis, residual stress measurements were made on several 207-size deep-groove ball bearings that were run for different time periods to determine a prestress cycle suitable for inducing significant compressive residual stresses in the inner-race-ball groove [57]. The results of this prestressing are shown in Fig. 20. Compressive residual stresses in excess of 0.69×10^9 N/m_2 (100 ksi) were included in the region of the maximum shearing stress in the bearing inner race run for 25 hr at a maximum Hertz stress of 3.3×10^9 N/m_2 (480 ksi) and a shaft speed of 2750 rpm. Twenty-seven bearings were prestressed for 25 hr at this condition and fatigue tested at a maximum Hertz stress of 2.4×10^9 n/M^2 (350 ksi). The results of these tests are shown in Fig. 21. The results of these tests are compared with results of baseline tests without a prestress cycle at identical test conditions. The 10-percent fatigue life of the prestressed ball bearings was greater than twice that of the baseline bearings. Additionally, from Fig. 22 the differences between the measured residual stress, is in the prestressed bearings and in the baseline bearings after 3000 to 4000 hr of testing are small [57].

RETAINED AUSTENITE

For three decades the effect of retained austenite on rolling-element fatigue has been openly discussed at technical meetings without the presentation of definitive data. In general, for a given through-hardened material, the amount of retained austenite generally increases with increasing material hardness. For case hardened materials, however, large amounts of retained austenite will be present in the case. It is well known that retained austenite will transform to martensite under Hertzian cyclic stress conditions and even at no load ambient conditions resulting in dimensional instability of the bearing component. For this reason, a low level of

retained austenite is desirable for critical bearing applications. Typical maximum levels are in the range of 2 to 5 percent. The effect of retained austenite cannot be easily separated from the effect of material hardness. For this reason, little work has been directed toward studying the effect of retained austenite on rolling-element fatigue.

It had been speculated that increased amounts of retained austenite can result in increased life if material hardness was maintained at a relative constant level. AMS 5749 steel, because of its alloy content, tends to retain higher levels of retained austenite, but levels as low as 5 percent are attainable with suitable heat treatment. This characteristic allows for development of test material with varied retained austenite while other characteristics such as hardness remain constant [58].

Rolling-element fatigue tests were conducted in the NASA five-ball fatigue tester with three lots of VIM-VAR AMS 5749 12.7-mm (1/2 in.) diameter balls at a maximum Hertz stress of 5.52×10^9 N/m^2 (800 ksi), a contact angle of 30°, and a shaft speed of 10 000 rpm at 339 K (150 °F). Each lot of the AMS 5749 had a different amount of retained austenite. The results of these tests are summarized in Figure 23 [58]. A comparison of the 10-percent lives of the three lots of VIM-VAR AMS 5749 does not present a clear effect of retained austenite on fatigue life. The intermediate level (lot B, 11.1 percent) gave the longest life with apparent statistical significance when compared with the highest level, where the confidence number is 97 percent, or greater than 2σ confidence. For the lowest level of retained austenite (lot C), the confidence number is 87 percent. Thus, it is apparent that the high level of retained austenite, 14.6 percent (lot A), is significantly detrimental to the 10-percent fatigue life. Therefore, an optimum level of retained austenite is suggested for maximum fatigue life. However, because of

the limits imposed by dimensional stability, such levels are probably not practical for bearings for critical applications such as in aircraft turbine engines.

It should be noted that an unusually high Weibull slope exists in the lot B failure distribution. The reason for this high slope along with the relatively long life of this lot is not understood; however, it is of interest to note that relatively early failures did not occur at the 11.1 percent retained austenite level. Thus, the 50-percent life data suggest a trend toward increased life with decreased retained austenite level. However, where high reliability is of importance, the main interest is in early failures, which is indicated best by the 10-percent life data [58].

Rolling-element fatigue tests were conducted with two rollers as specimens made from a carburized 18Cr2Ni4WA (0.18 percent C, 1.50 percent Cr, 4.25 percent NI, and 1.0 percent W) at a maximum Hertz stress of $3 \times 10^9 N/m^2$ (435 ksi) [59]. The rollers had retained austenite of 7, 12, 40, and 50 percent in the roller case. Hardness measurements were only reported for the 7 and 50 percent retained austenite rollers. These were maximum Vickers hardness of 800 and 730, respectively. While only three or four roller pairs were tested at each austenite level, there was a significant increase in fatigue life with increasing retained austenite. However, austenite does not appear independent of hardness. The results of this work shown in Fig. 24 suggest that the deformation-induced martensite transformation results in the creation of compressive residual stresses thus increasing life [59]. These results would also suggest that retained austenite may play more of a role in the results discussed previously relating hardness to life wherein induced compressive residual stresses are related in whole or in part to the transformation of the austenite into martensite. These transformations are

also related to metallurgical changes which have been previously reported [10]. Many investigators have sought a correlation of the so-called "white bands" in AISI 52100 induced during Hertzian contact with time and rolling-element fatigue. The "white bands" may be indicative of the residual stresses present due to the austenite transformation.

While retained austenite appears to improve rolling-element fatigue life, it can at the same time have a deleterious effect. It was reported in [60] and [61] that for tapered roller bearings made from AISI 4320 steel shallow surface distress was occurring on the raceway and roller taper surfaces. This type of distress is called peeling [61] and appears as a very shallow area, uniform in depth. Typical peeled areas in these bearings, approximately 0.008-mm (0.0003 in.) deep, are shown in Fig. 25. The peeling tended to initiate at minor surface defects such as deeper surface scratches or indentations [61].

The peeling also tended to be concentrated near the axial center of the raceways and roller with a slight bias toward the roller large end. This effect may be expected since the rollers are slightly crowned and the contact stress is somewhat higher in the center of the raceway. Profile traces across the raceways and along the roller tapers of the initial test bearings revealed that the roller crown radius had been decreased to approximately one-third of its original value. This exaggerated crown caused further stress concentration at the center of the roller and further aggravated the peeling [61].

This exaggerated crown was also observed in similar tests reported in [60] and was attributed to an uneven transformation of retained austenite. The level of retained austenite in the case of the AISI 4320 bearing steel is approximately 30 percent. Since austenite is a relatively unstable phase, it

transforms to martensite at a rate that depends on temperature and stress conditions. As it transforms, a growth of the material occurs. Since stresses and temperatures are higher near the center of the roller raceway contact due to higher Hertzian loading, greater transformation, and thus growth occurs there, and it becomes a self aggravating condition. Some measurements of retained austenite on the rollers from the initial test bearings indicated that nearly all of the austenite had transformed near the center. It is believed that the growth from this transformation could account for the exaggerated crown that was measured [61]. The cup and cone raceways also experienced some crown increase but to a lesser extent than the rollers [61].

Experience has shown that test rollers made from AISI 52100 of Rockwell C hardnesses greater than 63 will have sufficient austenite transform during rolling contact to alter the surface waviness and cause early spalling of the surfaces. Even for unrun bearings made from AISI M-50, growth of the bore of the inner ring can occur at room temperature with time where high amounts of retained austenite were initially present to render the bearing unfit for use.

FRACTURE TOUGHNESS

Table 5 lists both through-hardened and case-hardened bearing materials and their chemistry. It has been standard practice in the tapered roller bearing industry to manufacture tapered roller bearings from case-hardened steels. The reason for this is quite simple. Because of the higher loads which tapered roller bearings are subjected to, higher interference fits between the inner ring and shaft are required to prevent the ring from turning on the shaft. These higher interference fits induce rather high hoop (tensile) stresses in the ring which can result in fracture of the inner ring if through-hardened steels were used. Additionally, high thrust loads on the

flange of the tapered roller bearing can result in fracture failure of the flange if the flange were through hardened. As a result, through-hardened materials such as AISI 52100 and AISI M-50 have been rarely used for tapered roller bearing application. For temperatures under 608 K (300 °F) case hardened materials such as AISI 4320 and AISI 9310 have been commonly used. Within the last two decades, for higher temperature application, case carburized steels such as CBS 600, CBS 1000M, and VASCO X-2 have been used. Life tests were performed with 120.65-mm (4.75) bore tapered-roller bearings made from CVM AISI 4320 and CVM CBS 1000M at 12 500 rpm, a bearing temperature of 391 K (245 °F), a thrust load of 53 400 N (12 000 lb), and a radial load of 26 700 N (6000 lb) [61]. Twelve bearings of the AISI 4320 material ran to a 1100-hr cutoff time without failure of any type. At these conditions the rated catalog life of this bearing design is 102 hr, so that the experimental 10-percent life is greater than 10 times the catalog life [61].

Sixteen bearings made from CVM CBS 1000M material were run to spalling fatigue failure or to the 1100-hr cutoff time. Twelve of the bearings ran to 1100 hr without failure. Three bearings experienced spalls on the cup or cone raceways. One bearing was suspended at 820 hours without spalling failure. Based on the three failed bearings, the life of the CBS 1000M bearings was estimated to be 600 hr, or about six times the rated catalog life [61].

A comparison of the results of the two materials showed that the CVM CBS 1000M bearing life is less than the AISI 4320 bearing life. However, a quantitative estimate of the difference was not possible from these results since no fatigue failures occurred with the AISI 4320 bearings. Metallurgical analysis of the CBS 1000M bearings revealed that the cup and cone materials had coarser than desired grain structure. These bearings were made from the

first heat of the material and were exposed to forging temperatures later found to be excessive. In general, prior austenite grain size should be ASTM 8 or finer and individual grains should not exceed ASTM 15 [1].

Ten tapered roller bearings of a modified design made from VIM-VAR AISI M-50 steel were run at the same loads as the AISI 4320 and CBS 1000M bearings but at a speed of 18 500 rpm. The rated catalog life for these bearings was 46 hr. For various reasons related to rig malfunction, testing of six of these 10 bearings were suspended before the cutoff time of 1100 hr. Two bearings reached the 1100-hr cutoff time without failure. Two bearings developed cracked cones after 188 hours.

The average tangential tensile hoop stress, based on the assumption of thin rings, was estimated for the 18 500-rpm condition to be approximately $0.145 \times 10^9 N/m^2$ (21 000 psi). This calculated stress also includes effects of the cone-shaft interference fit. This stress is at the lower end of the range where critical crack size can be readily reached in through hardened steel [61].

For ball and cylindrical roller bearings through hardened steels are commonly used. Most of these bearings are run at speeds less than 2 million DN with some bearings in main shaft turbojet engine applications running at 2.2 million DN. As engine speeds increase to achieve improved efficiency and better specific fuel consumption, bearing speed will also increase. It is expected that bearing speeds will approach 3 million in the next decade. At bearing speeds greater than 2.3 million DN, bearings using conventional through-hardened bearing steels such as AISI 52100, AISI M-50, or 18-4-1 (AISI T-1), will be subject to race fracture either independently or as a result of a fatigue spall. This was graphically illustrated in the test reported in [8] with a 120-mm bore angular-contact ball bearing run at

3 million DN in which a defect was induced at the bearing inner race to cause spalling. The expected inner-race spalling at the induced defect occurred after 6 hr and 17 min. Testing was continued until an obvious severe fragmentation fracture occurred to the inner ring, terminating the test, 7.5 min after detection of the spalling (Fig. 26). Post-test examination showed that the inner ring had fractured into eight discrete segments [8].

From these tests it became obvious that, as with tapered roller bearings, materials with improved fracture toughness, e.g., case carburized steels, must be used. Comparison of the fatigue lives of CVM AISI M-50, CVM AISI 9310, and CBS 600 in the RC fatigue tester at $4.8 \times 10^9 N/m^2$ (700 ksi) are shown in Fig. 27. The AISI 9310 and CBS 600 had equivalent fatigue lives to the AISI M-50 [17]. However, materials such as AISI 9310 do not maintain their hot hardness while materials such as CBS 600 require much more quality assurance and control during processing to achieve the required rolling-element fatigue life.

Fracture toughness of a material is inversely proportional to carbon content and hardness. The amount of carbon present also determines hardness. A means of improving the fracture toughness without affecting hardness is to add nickel. When present in high-chromium, low-carbon steels, nickel causes the steel to become fully austenitic at temperatures above 1359 K (1650 °F), where the steel is heat treated or carburized. This also influences carbide size and distribution within the steel which affects fatigue life.

Recognizing the above, E.N. Bamberger, at the General Electric Co. [9], modified the chemistry of AISI M-50 steel by decreasing the amount of carbon and increasing the amount of nickel [9]. He called this modified material M-50NiL (the Ni referring to increased nickel and the L to low carbon).

The M-50NiL which is case carburized has a core which has a fracture toughness KI_c of over 60 MPa $\sqrt{m}$ (50 ksi $\sqrt{in.}$) and an average core hardness of Rockwell C 43 to 45 as compared to AISI M-50 of 29 MPa $\sqrt{m}$ (20 ksi $\sqrt{in.}$) [62]. The carbide structure of M-50NiL, shown in Figure 28, has fine carbides (compounds of carbon and various alloying elements) dispersed evenly within the steel's microstructure as compared to the courser carbides found in the standard AISI M-50 [62].

Compressive residual stresses on the order of $0.2 \times 10^9 N/m^2$ (30ksi) are induced in the zone of maximum resolved shearing stresses during the carburization process [62]. These residual stresses combined with the fine carbide structure will improve the rolling-element fatigue life of the material over conventional AISI M-50. This is illustrated by the rolling-element fatigue test results of the RC fatigue tester (Fig. 29) which compares standard VIM-VAR AISI M-50 and VIM-VAR M-50NiL. The M-50NiL had a 10-percent fatigue life of over twice that of the standard AISI M-50 [9]. Bearing tests reported in [9] show that under conditions which resulted in fracture of standard AISI M-50 inner races, bearing races made from M-50NiL and selected carburized steels did not show any signs of incipient fracture or even a tendency to fracture. This assures that bearing steel requirements for the next decade and beyond can be met by these most recent carburized materials.

CONCLUSION

During the last four decades, significant technical advancements in the bearing and steel industry have allowed for the design and manufacture of rolling-element bearings having lives over 100 times that which could be achieved in the 1940's and at speeds to 3 million DN. The results of these achievements can be catagorized into improved material cleanliness, controlled

material hardness, smaller and evenly dispersed carbide structure, induced compressive residual stresses, and improved fracture toughness. While the effect of material grain size was not discussed, it is generally accepted in the bearing industry that prior austenite grain size should be ASTM number 8 or finer and individual grains should not exceed ASTM number 5. It is further apparent that the chemical composition of a bearing steel does not have the affect on material hot hardness or life that it once was thought to have. What appears to be of paramount importance is the steel melting process such as VIM-VAR and an optimized heat treating process, together with its related process controls, in order to achieve a uniform and consistent end product. The vast differences which were once thought to distinguish through-hardened materials from case carburized materials really never existed but resolves to differences in fracture toughness necessary for either highly loaded and/or very high-speed applications. Case carburized M-50NiL appears to incorporate all the desirable qualities discussed herein into a material whereby optimal life and reliability can be achieved not only for current bearing applications but for those of the next decade and beyond.

REFERENCES

[1] Irwin, A.S., Anderson, W.J., and Derner, W.J., "Review and Critical Analysis-Rolling-Element Bearings for System Life and Reliability," NASA CR-174710, NASA, Washington, D.C., 1985.

[2] Dowson, D. and Higginson, G.R., Elasto Hydrodynamic Lubrication, Pergamon Press, Oxford, 1966.

[3] Grubin, A.N., "Fundamentals of the Hydrodynamic Theory of Lubrication of Heavily Loaded Cylindrical Surfaces," Investigation of the Contact of Machine Components, Kh.F. Ketova, Ed., Translation of Russian Book, no. 30, Central Scientific Institute for Technology and Mechanical Engineering, Moscow, 1949, Chapter 2, (Available from Department of Scientific and Industrial Research, Great Britain, Transl. CTS-235, and Special Libraries Association, Transl. R-3554.)

[4] Bamberger, E.N., Zaretsky, E.V., and Anderson, W.J., Journal of Lubrication Technology, Vol. 92, No. 1, Jan. 1970, pp. 23-33.

[5] Bear, H.R. and Butler, R.H., "Preliminary Metallographic Studies of Ball Fatigue Under Rolling-Contact of Conditions," NACA TN-3925, National Advisory Committee for Aeronautics, Washington, D.C., 1957.

[6] Carter, T.L., Butler, R.H., Bear, H.R., and Anderson, W.J, ASLE Transactions, Vol. 1, No. 1, 1958, pp. 23-32.

[7] Zaretsky, E.V., Parker, R.J., and Anderson, W.J., "Effect of Component Differential Hardnesses on Rolling-Contact Fatigue and Load Capacity," NASA TN D-2640, NASA, Washington, D.C., 1965.

[8] Bamberger, E.N., Zaretsky, E.V., and Signer, H., Journal of Lubrication Technology, Vol. 98, No. 4, Oct. 1976, pp. 580-585.

[9] Bamberger, E.N., in Tribology in the 80's, W.F. Loomis, Ed., NASA CP-2300, Vol. 2, 1983, pp. 773-794.

[10] Carter, T.L., "A Study of Some Factors Affecting Rolling-Contact Fatigue Life," NASA TR-R-60, NASA, Washington, D.C., 1960.

[11] Jones, A.B., in Symposium on Testing of Bearings, ASTM, 1947, pp. 35-52.

[12] Johnson, R.F., and Sewell, J.F., Journal of the Iron and Steel Institute, Vol. 196, Pt. 4, 1960, pp. 414-444.

[13] Given, P.S., "Chemical Analysis Variation and Melting Practices," Panel Session, Achievements in AFMA Calculated Bearing Life, ASME Spring Lubrication Conference, June 1963.

[14] Morrison, T.W., Tallian, T., Walp, H.O., and Baile, G.H., ASLE Transactions, Vol. 5, No. 2, Nov. 1962, pp. 347-364.

[15] Zaretsky, E.V. and Bamberger, E.N., "Advanced Airbreathing Engine Lubricants Study with a Tetraester Fluid and a Synthetic Paraffinic Oil at 492K (425°F), " NASA TN D-6771, NASA, Washington, D.C., 1972.

[16] Bamberger, E.N., et. al., Life Adjustment Factors for Ball and Roller Bearings, An Engineering Design Guide, ASME, New York, 1971.

[17] Nahm, A.H., in Advanced Power Transmission Technology, G.K. Fischer, Ed., NASA CP-2210, 1983, pp. 173-184.

[18] Parker, R.J. and Hodder, R.S., Journal of Lubrication Technology, Vol. 100, No. 2, Apr. 1978, pp. 226-235.

[19] Koved, I., Rospond, R.T., "Detection of Potential Fatigue Nuclei in Rolling Contact Bearings," SAE Paper No. 893B, Sept. 1964.

[20] Carter, T.L., Zaretsky, E.V., and Anderson, W.J., "Effect of Hardness and Other Mechanical Properties on Rolling-Contact Fatigue Life of Four High-Temperature Bearing Steels," NASA TN D-270, NASA, Washington, D.C., 1960.

[21] Jackson, E.R., ASLE Transactions, Vol. 2, No. 1, 1959, pp. 121-128.

[22] Baughman, R.A., Journal of Basic Enginering, Vol. 82, No. 2, June 1960, pp. 287-294.

[23] Chevalier, J.L., Dietrich, M.W., and Zaretsky, E.V., "Short-Term Hot Hardness Characteristics of Rolling-Element Steels," NASA TN D-6632, NASA, Washington, D.C., 1972.

[24] Chevalier, J.L., Dietrich, M.W., and Zaretsky, E.V., "Hot Hardness Characteristics of Ausformed AISI M-50, Matrix II, WD-65, Modified 440-C, and Super Nitralloy," NASA TN D-7244, NASA, Washington, D.C., 1973.

[25] Anderson, N.E. and Zaretsky, E.V., "Short-Term Hot-Hardness Characteristics of Five Case Hardened Steels," NASA TN D-8031, NASA, Washington, D.C., 1975.

[26] Palmgren, A., Ball and Roller Bearing Engineering, 3rd. ed., SKF Industries, Philadelphia, PA., 1959, pp. 73-82.

[27] Anderson, N.E., "Long-Term Hot-Hardness Characteristics of Five Through-Hardened Bearing Steels," NASA TP-1341, NASA, Washington, D.C., 1978.

[28] Zaretsky, E.V., Parker, R.J., and Anderson, W.J., Journal of Lubrication Technology, Vol. 89, No. 1, Jan. 1967, pp. 47-62.

[29] Zaretsky, E.V., Parker, R.J., Anderson, W.J., and Reichard, D.W., "Bearing Life and Failure Distribution as Affected by Actual Component Differential Hardness," NASA TN D-3101, NASA, Washington, D.C., 1965.

[30] Irwin, A.S., "Effect of Bearing Temperatures on Capacities of Bearings of Various Materials," Paper presented at ASME Third Spring Lubrication Symposium, New York, N.Y., Mar. 14-15, 1960.

[31] Parker, R.J., Zaretsky, E.V., and Dietrich, M.W., "Rolling-Element Fatigue Lives of Four M-Series Steels and AISI 52100 at 150°F," NASA TN D-7033, NASA, Washington, D.C., 1971.

[32] Parker, R.J., Zaretsky, E.V., and Dietrich, M.W., "Rolling-Element Fatigue Lives of AISI T-1, AISI M-42, AISI 52100, and Halmo at 150°F," NASA TN D-6179, NASA, Washington, D.C., 1971.

[33] Parker, R.J. and Zaretsky, E.V., Journal of Lubrication Technology, Vol. 94, No. 2, Apr. 1972, pp. 165-173.

[34] Chevalier, J.L. and Zaretsky, E.V., "Effect of Carbide Size, Area, and Density on Rolling-Element Fatigue," NASA TN D-6835, NASA, Washington, D.C., 1972.

[35] Chevalier, J.L., Zaretsky, E.V., and Parker, R.J., Journal of Lubrication Technology, Vol. 95, No. 3, July 1973, pp. 287-293.

[36] Parker, R.J. and Bamberger, E.N., "Effect of Carbide Distribution on Rolling-Element Fatigue Life of AMS 5749," NASA TP-2189, NASA, Washington, D.C., 1983.

[37] Bamberger, E.N., Journal of Lubrication Technology, Vol. 89., No. 1, Jan. 1967, pp. 63-75.

[38] Bamberger, E.N., "The Production, Testing and Evaluation of Ausformed Ball Bearings," NOW-65-0070-F, General Electric Co., Cincinnati, Oh, June 1966.

[39] Parker, R.J. and Zaretsky, E.V., "Rolling-Element Fatigue Life of Ausformed M-50 Steel Balls," NASA TN D-4954, NASA, Washington, D.C., 1968.

[40] Hopkins, J.M. and Johnson, J.H., "Method of Producing Improved Bearing Components by Elimination or Control of Fiber Orientation," NASA CR-55402, Nov. 1963.

[41] Zaretsky, E.V., Machine Design, Vol. 38, No. 24, Oct. 13, 1966, pp. 206-223.

[42] Zaretsky, E.V., Parker, R.J., Anderson, W.J., and Miller, S.T., "Effect of Component Differential Hardness on Residual Stress and Rolling-Contact Fatigue," NASA TN D-2664, NASA, Washington, D.C., 1965.

[43] Cioclov, D., Journal of Lubrication Technology, Vol. 91, No. 2, Apr. 1969, pp. 290-291.

[44] Foord, C.A., Hingley, C.G., and Cameron, A., Journal of Lubrication Technology, Vol. 91, No. 2, Apr. 1969, pp. 282-293.

[45] Lundberg, G., and Palmgren, A., Acta Polytechnica Mechanical Engineering Series, Vol. 1, No. 3, 1947, pp. 1-50.

[46] Zaretsky, E.V., Parker, R.J. and Anderson, W.J., Journal of Lubrication Technology, Vol. 91, No. 2, Apr. 1969, pp. 314-319.

[47] Akaoka, J., Rolling Contact Phenomena, J.B. Bidwell, Ed., Elsevier, 1962, pp. 266-300.

[48] Gentile, A.J., and Martin, A.D., "The Effect of Prior Metallurgically Induced Compressive Residual Stress on the Metallurgical and Endurance Properties of Overload Tested Ball Bearings," ASME Paper 65-WA/CF-7, Nov. 1965.

[49] Scott, R.L., Kepple, R.K., and Miller, M.H., in Rolling Contact Phenomena, J.B. Bidwell, Ed., Elsevier, 1962, pp. 301-316.

[50] Koistinen, D.P., ASM Transactions, Vol. 57, 1964, pp. 581-588.

[51] Stickels, C.A., and Janotik, A.M., Metallurgical Transactions A, Vol. 11, No. 3, Mar. 1980, pp. 467-473.

[52] Naisong, Xu, Stickels, C.A., and Peters, C.R., Metallurgical Transactions A, Vol. 15, No. 11, Nov. 1984, pp. 2101-2102.

[53] Bush, J.J., Grube, W.L., and Robinson, G.H., in Rolling Contact Phenomena, J.B. Bidwell, Ed., Elsevier, 1962, pp. 400-424.

[54] Almen, J.O., in Rolling Contact Phenomena, J.B. Bidwell, Ed., Elsevier, 1962, pp. 400-424.

[55] Gentile, A.J., Jordan, E.F., and Martin, A.D., AIME Transactions, Vol. 233, No. 6, June 1965, pp. 1085-1093.

[56] Muro, H., and Tsushima, N., Wear, Vol. 15, 1970, pp. 309-330.

[57] Parker, R.J., and Zaretsky, E.V., "Effect of Residual Stresses Induced by Prestressing on Rolling-Element Fatigue Life," NASA TN D-6995, NASA, Washington, D.C., 1972.

[58] Parker, R.J. and Hodder, R.S., "Effect of Double Vacuum Melting and Retained Austenite on Rolling-Element Fatigue Life of AMS 5749 Bearing Steel," NASA TP-1060, NASA, Washington, D.C., 1977.

[59] Dong, Z., Fu-Zing, W., Qi-Gong, C., Ming-Xin, Z., and Yin-Quian, C., Wear, Vol. 105, 1985, pp. 223-234.

[60] Lenski, J.W., Jr., "Test Results Report and Design Technology Development Report. HLH/ATC High-Speed Tapered Roller Bearing Development Program," T301-10248-1, Boeing Vertol Co., Philadelphia, PA, June 1974, (USAAMRDL-TR-74-33).

[61] Parker, R.J., Signer, H.R., and Pinel, S.I., Journal of Lubrication Technology, Vol. 104, No. 3, July 1982, pp. 293-299.

[62] Philip, T.V., Power Transmission Design, Vol. 28, June 1986, pp. 43-46.

TABLE 1. - SUMMARY OF ENDURANCE TESTS WITH 120-MM BORE ANGULAR CONTACT BALL BEARINGS

[Material, VIM-VAR AISI M-50 Steel; Temperature, 492 K (425 °F); Contact angle, 24°.]

Speed rpm (DN)	Thrust load, N (lb)	Maximum Hertz stress, N/m^2 (ksi)		Predicted life[a] rev.x10^{-6} (hr)		Experimental life, rev.x10^{-6} (hr)		Experimental Weibull slope	Failure index[c]
		Inner race	Outer race	L_{10}	L_{50}	L_{10}	L_{50}		
12 000 ($1.44x10^6$)	66 721 (5000)	$2048x10^6$ (297)	$1731x10^6$ (251)	29 (40)	157 (216)	[b]2700 (3750)	[b]6975 (9687)	[b]2.1	1 out of 30
25 000 ($3.0x10^6$)	66 721 (5000)	$1965x10^6$ (285)	$2096x10^6$ (304)	21 (14)	113 (76)	2400 (1600)	6200 (4133)	2.1	6 out of 30

[a]Centrifugal effects included.
[b]Estimated.
[c]Indicates number of failures out of total number of tests.

TABLE 2. - TEMPERATURE PROPORTIONALITY FACTORS α AND EXPONENTS β FOR BEARING STEELS

$[(Rc)_T = (Rc)_{RT} - \alpha \Delta T^{\beta}.]$

Material	Temperature range		α		β	
	K	°F	K	°F	K	°F
AISI 8620	294 to 589	70 to 600	73×10^{-5}	26×10^{-5}	1.7	1.7
CBS 600	294 to 589	70 to 600	0.75×10^{-5}	0.18×10^{-5}	2.4	2.4
Vasco X-2	294 to 811	70 to 1000	1.4×10^{-5}	0.38×10^{-5}	2.2	2.2
CBS 1000	294 to 811	70 to 1000	93×10^{-5}	38×10^{-5}	1.5	1.5
CBS 1000M	294 to 811	70 to 1000	340×10^{-5}	160×10^{-5}	1.3	1.3
SUPER NITRALLOY	294 to 769	70 to 620	1.3×10^{-5}	0.33×10^{-5}	2.3	2.3
AISI 52100	294 to 533	70 to 500	92×10^{-5}	34×10^{-5}	1.6	1.6
AISI M-50	294 to 811	70 to 1000	133×10^{-5}	54×10^{-5}	1.4	1.4
AISI M-1	294 to 811	70 to 1000	133×10^{-5}	54×10^{-5}	1.4	1.4
AISI M-2	294 to 811	70 to 1000	133×10^{-5}	54×10^{-5}	1.4	1.4
AISI M-10	294 to 811	70 to 1000	133×10^{-5}	54×10^{-5}	1.4	1.4
AISI M-42	294 to 811	70 to 1000	133×10^{-5}	54×10^{-5}	1.4	1.4
AISI T-1 (18-4-1)	294 to 811	70 to 1000	133×10^{-5}	54×10^{-5}	1.4	1.4
Halmo	294 to 811	70 to 1000	133×10^{-5}	54×10^{-5}	1.4	1.4
WB-49	294 to 811	70 to 1000	133×10^{-5}	54×10^{-5}	1.4	1.4
WD-65	294 to 811	70 to 1000	133×10^{-5}	54×10^{-5}	1.4	1.4
Matrix II	294 to 811	70 to 1000	133×10^{-5}	54×10^{-5}	1.4	1.4
AISI 440C	294 to 811	70 to 1000	133×10^{-5}	54×10^{-5}	1.4	1.4
AMS 5749	294 to 811	70 to 1000	133×10^{-5}	54×10^{-5}	1.4	1.4
M-50NiL	294 to 811	70 to 1000	133×10^{-5}	54×10^{-5}	1.4	1.4

TABLE 3. - HARDNESS OF AISI 52100 STEEL INITIALLY HARDENED TO THREE HARDNESS VALUES (R_C 60.5, R_C 62.5, AND R_C 64.5) AFTER EXPOSURE TO INDICATED SOAK TEMPERATURES FOR 100 AND 500 HOURS

Soak temperature		Time at soak temperature, hr			
K	°F	100	500 to 1000	100	500 to 1000
		Room-temperature hardness (R_C at 297 K (75 °F))		Hot hardness (R_C at soak temperature)	
366	200	[a]	[a]	[a]	[a]
394	250	[b]63.2	[b]61.5	[b]62.1	[b]61.2
422	300	61.0	60.0	60.0	58.8
450–478	350–400	60.0	58.7	58.0	56.5

[a]No change from initial values.
[b]Maximum value attainable; if initial hardness is below this value, time at this temperature will have no effect.

TABLE 4. - FATIGUE RESULTS WITH GROUPS OF 12.7 MM (1/2 IN.) DIAMETER BALLS RUN IN FIVE-BALL FATIGUE TESTERS. MAXIMUM HERTZ STRESS, $5.5 \times 10^9 N/m^2$ (800 000 PSI); CONTACT ANGLE, 30°, SHAFT SPEED, 10 300 RPM; RACE TEMPERATURE, 534 K (150 °F)

Material	Heat treatment lot	Average hardness, R_C	Retained austenite, volume percent[a]	Austenitic grain size[b]	Cleanliness rating[c]		Life, millions of upper ball stress cycles		Slope	Failure index[e]	Carbide factor C'
					Class[d]	Type	L_{10}	L_{50}			
52100	A	62.5	4.90	13	B1	Heavy	18.5	114	1.04	22 out of 29	1.22
	B	62.0	4.10	13	D1	Thin	30.1	130	1.29	22 out of 29	1.17
	C	62.5	.80	13	D1	Thin	12.9	84	1.00	19 out of 25	.76
	Combined	----	----	--	--	-----	21.2	109	1.15	63 out of 83	1.00
Halmo	A	60.8	0.60	8	D2	Heavy	22.0	74	1.56	25 out of 30	0.58
	B	60.8	1.00	8	D1	Heavy	12.9	57	1.26	28 out of 30	.64
	C	61.1	1.70	8	D2	Heavy	12.9	68	1.14	26 out of 30	.69
	Combined	----	----	--	--	-----	16.4	66	1.35	79 out of 90	.63
M-50	A	62.6	1.90	10	B1	Heavy	15.3	35	2.29	29 out of 29	0.60
	B	62.2	2.90	9	D2	Heavy	12.3	36	1.73	24 out of 30	.54
	C	62.3	1.50	10	D1	Heavy	14.2	48	1.55	26 out of 29	.50
	Combined	----	----	--	--	-----	14.4	39	1.89	79 out of 88	.56
M-10	A	62.2	1.10	9	D3	Heavy	19.4	65	1.56	26 out of 30	0.36
	B	62.0	2.40	6	D2	Heavy	8.3	46	1.11	30 out of 30	.39
	C	61.8	1.60	6	D1	Thin	13.1	42	1.62	29 out of 30	.35
	Combined	----	----	--	--	-----	13.2	50	1.40	85 out of 90	.37
T-1	A	61.4	7.30	11	B1	Heavy	6.6	50	0.92	26 out of 30	0.26
	B	61.4	5.20	9	D1	Thin	8.4	59	.97	26 out of 30	.33
	C	61.0	9.50	10	D1	Heavy	8.5	74	.87	23 out of 30	.30
	Combined	----	----	--	--	-----	8.6	59	.98	75 out of 90	.29
M-1	A	63.3	2.90	10	B2	Heavy	8.2	43	1.13	29 out of 30	0.32
	B	63.4	3.30	9	A1	Heavy	5.9	37	1.02	29 out of 30	.34
	C	63.5	1.00	8	A2	Heavy	6.7	33	1.18	29 out of 29	.38
	Combined	----	----	--	--	-----	7.6	38	1.18	87 out of 89	.33
M-2	A	63.4	1.70	6	B1	Heavy	5.8	35	1.05	28 out of 30	0.36
	B	63.4	2.40	10	D1	Thin	5.5	26	1.23	28 out of 29	.36
	C	63.4	2.30	9	D1	Heavy	4.2	31	.95	29 out of 30	.35
	Combined	----	----	--	--	-----	5.7	30	1.13	85 out of 89	.36
M-42	A	61.8	1.00	9	A1	Thin	1.0	6.6	0.97	30 out of 30	0.07
	B	61.3	4.40	10	D1	Heavy	1.7	8.9	1.12	27 out of 30	.07
	C	61.3	4.90	8	D1	Heavy	1.4	5.8	1.33	30 out of 30	.07
	Combined	----	----	--	--	-----	1.4	7.0	1.18	87 out of 90	.07

[a]Determined from the integrated peak intensities of $(220)_\gamma$ and $(200)_\alpha$ planes.
[b]ASTM E 112-63.
[c]ASTM E45 63, Method A (table shows predominate inclusion class and type).
[d]Inclusion classes: A-Sulfides, B-Alumina, C-Silicates, D-Globular oxides.
[e]Indicates number of failures out of total number of tests.

TABLE 5. - CHEMICAL COMPOSITION OF BEARING STEELS

Material	Alloying Element, Percent by Weight (Balance Fe)												
	C	P(max)	S(max)	Mn	Si	Cr	V	W	Mo	Co	Cb	Ni	Other
AISI 52100	1.00	0.025	0.025	0.35	0.30	1.45	----	----	----	----	----	----	------
MHT	1.03	.025	.025	.35	.35	1.50	----	----	----	----	----	----	1.36Al
HALMO	.56	.003	.008	.36	1.12	4.84	0.53	----	5.18	----	----	----	------
AISI M-1	.80	.030	.030	.30	.30	4.00	1.00	1.50	8.00	----	----	----	------
AISI M-2	.83	.030	.030	.30	.30	3.85	1.90	6.15	5.00	----	----	----	------
AISI M-10	.85	.030	.030	.25	.30	4.00	2.00	----	8.00	----	----	----	------
AISI M-42	1.10	.012	.007	.15	.17	3.77	1.15	1.66	9.51	7.99	----	----	------
AISI M-50	.80	.030	.030	.30	.25	4.00	1.00	----	4.25	----	----	----	------
T-1 (18-4-1)	.70	.030	.030	.30	.25	4.00	1.00	18.0	----	----	----	----	------
T-15	1.52	.010	.004	.26	.25	4.70	4.90	12.5	.20	5.10	----	----	------
440C	1.03	.018	.014	.48	.41	17.30	.14	----	.50	----	----	----	------
AMS 5749	1.15	.012	.004	.50	.30	14.50	1.20	----	4.00	----	----	----	------
Vasco Matrix II	.53	014	013	.12	.21	4.13	1.08	1.40	4.80	7.81	----	0.10	------
CRB-7	1.10	.016	.003	.43	.31	14.00	1.03	----	2.02	----	0.32	----	------
AMS 5900	1.10	.014	.007	.40	.30	14.00	1.0	----	2.0	----	----	----	.25Nb
AISI 9310 (C)	.10	.006	.001	.54	.28	1.18	----	----	.11	----	----	3.15	------
CBS 600 (C)	.19	.007	.014	.61	1.05	1.50	----	----	.94	----	----	.18	------
CBS 1000M (C)	.14	.018	.019	.48	.43	1.12	----	----	4.77	----	----	2.94	------
VASCO X-2 (C)	.14	.011	.011	.24	.94	4.76	.45	1.40	1.40	.03	----	.10	------
Bower 315 (C)	.13	-----	-----	.50	----	1.55	----	----	5.00	----	----	2.80	------
AISI 8620 (C)	.21	-----	-----	.80	----	.50	----	----	.20	----	----	.55	------
AISI 3310 (C)	.11	-----	-----	.52	----	1.58	----	----	----	----	----	3.50	------
AISI 4320 (C)	.20	-----	-----	.55	----	.50	----	----	.25	----	----	1.82	------
AISI 4620 (C)	.20	-----	-----	.55	----	-----	----	----	.25	----	----	1.82	------
AISI 4720 (C)	.20	-----	-----	.55	----	.45	----	----	.20	----	----	1.05	------
M-50 NiL (C)	.13	.030	.030	.30	.25	4.00	1.20	----	4.25	----	----	3.50	------

(C) Carburizing Grades

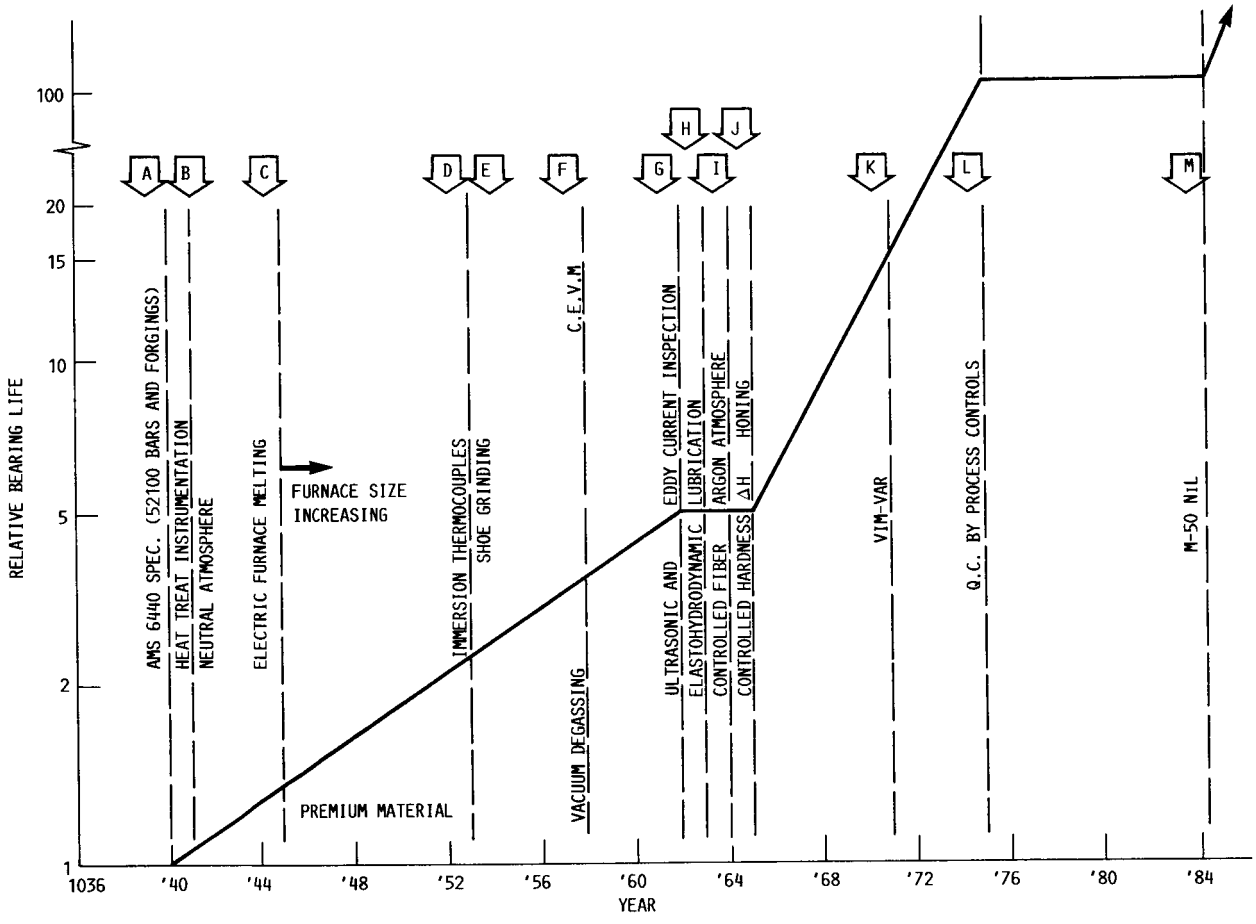

FIGURE 1.- MAJOR ADVANCES CONTRIBUTING TO ROLLING-ELEMENT BEARING LIFE IMPROVEMENT OVER THE PAST FOUR DECADES.

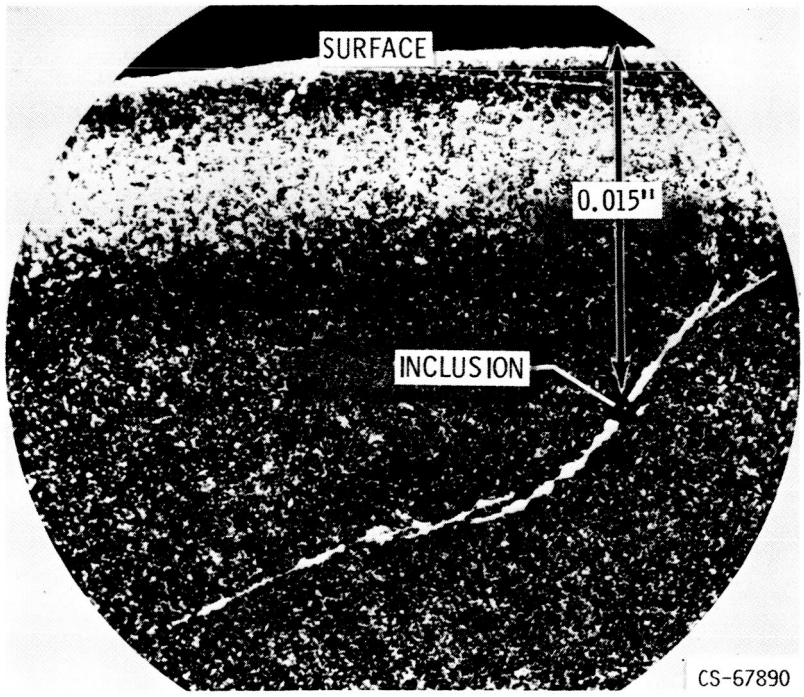

FIGURE 2. - FATIGUE CRACK EMANATING FROM AN INCLUSION.

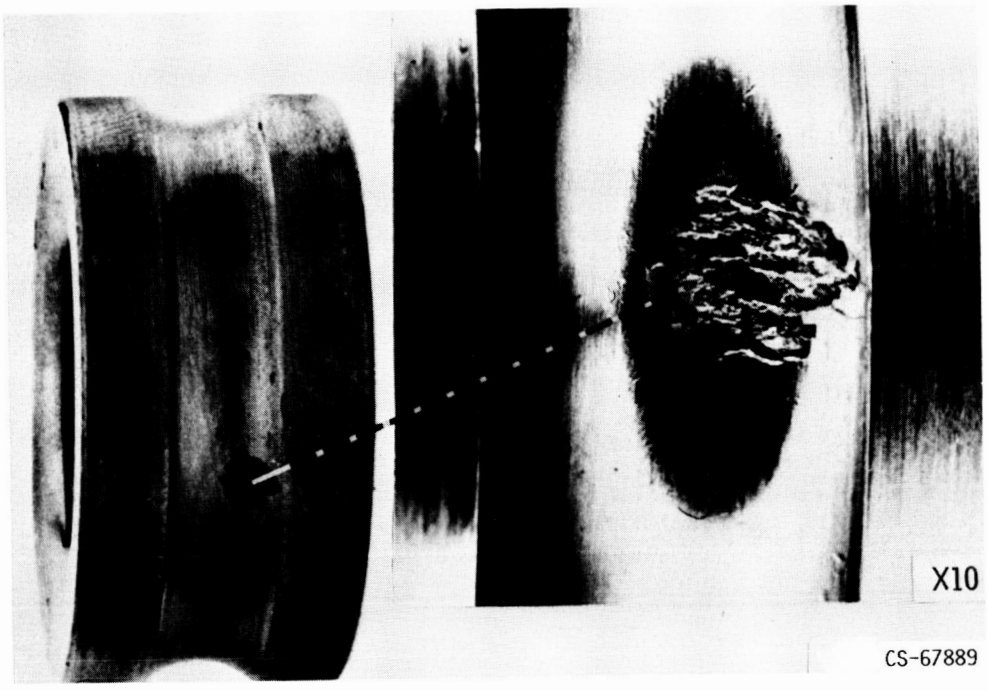

FIGURE 3. - TYPICAL FATIGUE SPALL IN BEARING RACE.

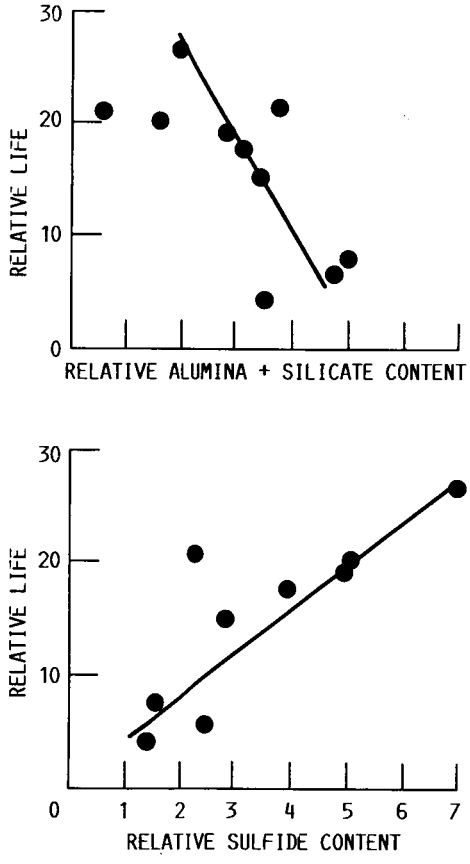

FIGURE 4.- RELATIONSHIP BETWEEN LIFE AND INCLUSION CONTENT.

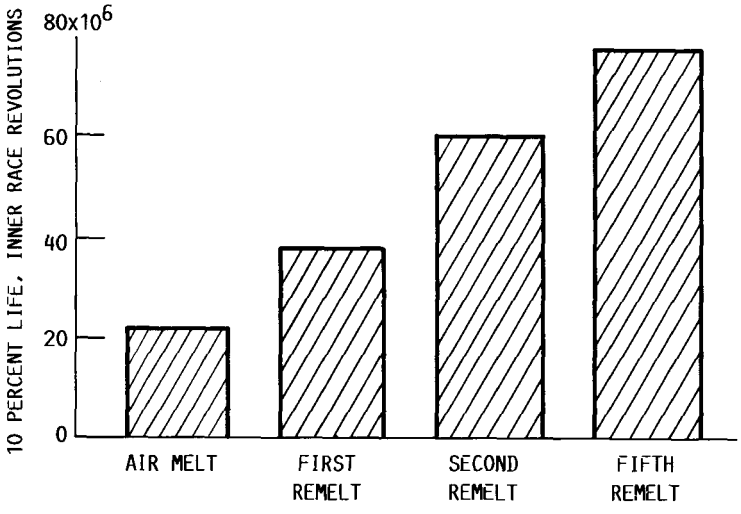

FIGURE 5.- LIFE OF 6309-SIZE BEARING INNER RACES MADE FROM AIR MELT AND SUCCESSIVE CONSUMABLE REMELTS OF THE SAME HEAT AISI 52100 STEEL.

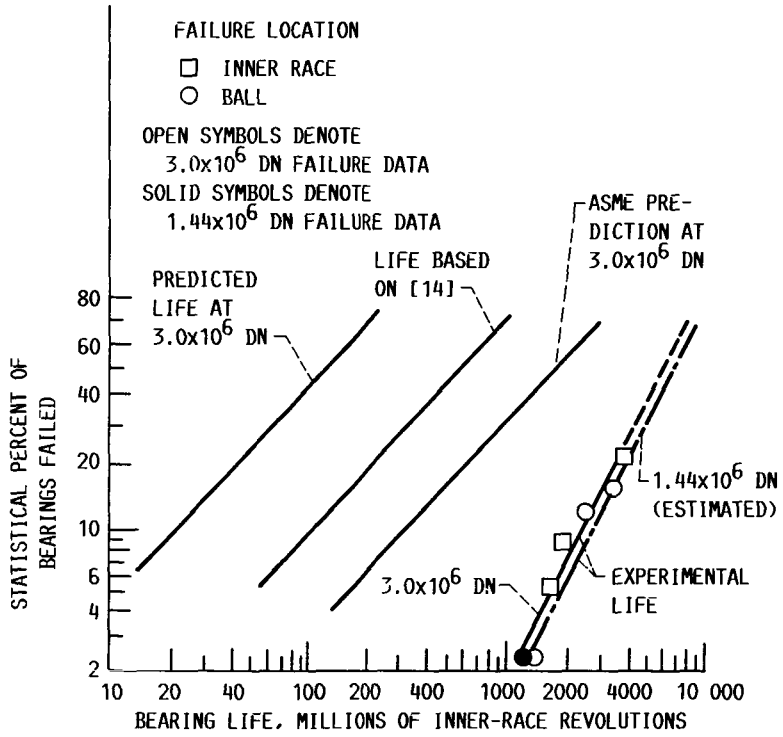

FIGURE 6.- ENDURANCE CHARACTERISTICS OF 120-MM BORE ANGULAR-CONTACT BALL BEARINGS. THRUST LOAD, 22 241 N (5000 LB); TEMPERATURE, 492 K (425 ^{0}F); MATERIAL VIM-VAR AISI M-50 STEEL; LUBRICANT, TETRAESTER.

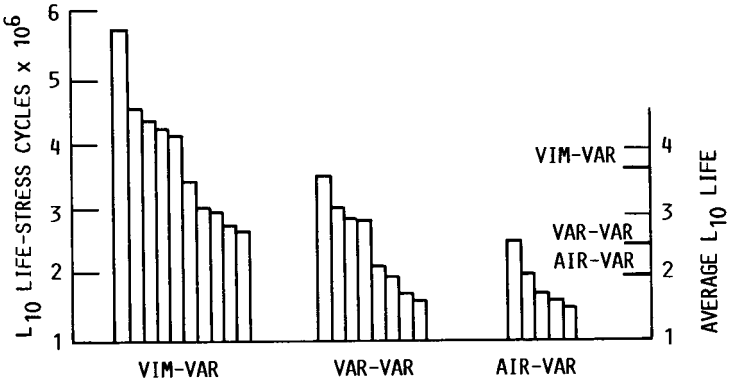

FIGURE 7.- ROLLING-CONTACT (RC) RIG EVALUATION OF AISI M-50 MELTING PROCEDURES. (EACH BAR REPRESENTS 20 TESTS).

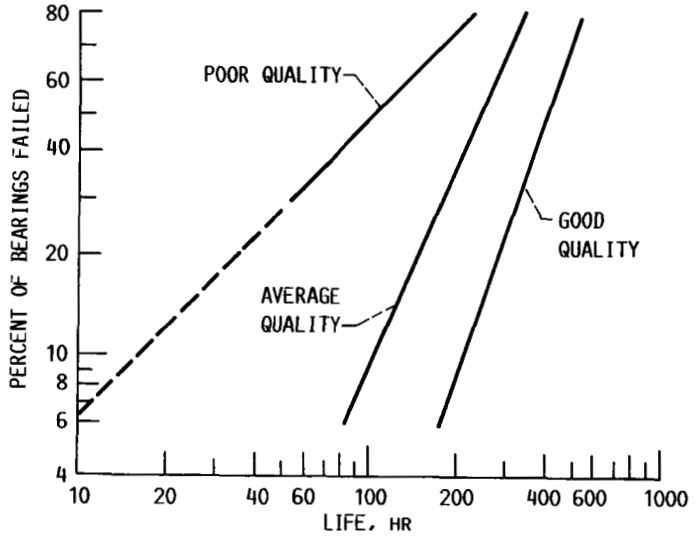

FIGURE 8.- FATIGUE LIFE DISTRIBUTION OF 309-SIZE ROLLER BEARINGS MADE FROM AISI 8620 STEEL GROUPED INTO THREE QUALITY RATINGS BASED ON ULTRASONIC RESPONSE.

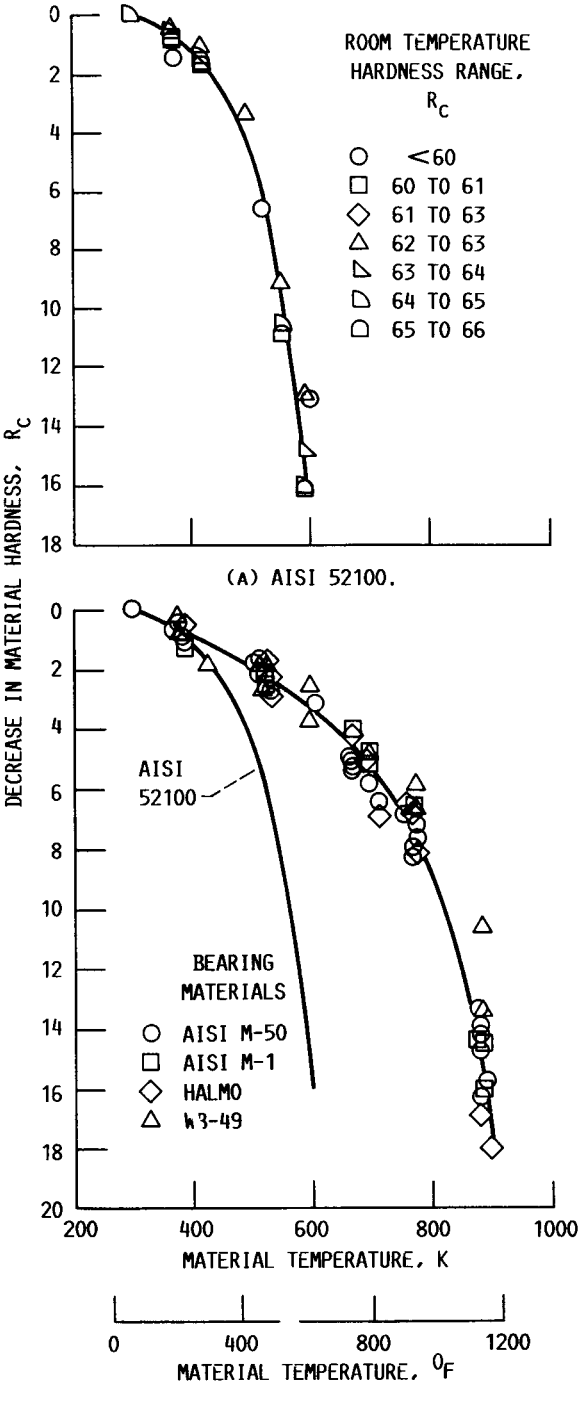

(A) AISI 52100.

(B) COMBINED NORMALIZED SHORT-TERM HARDNESS FOR HIGH-TEMPERATURE THROUGH HARDENDED BEARING STEELS.

FIGURE 9.- SUMMARY OF SHORT-TERM HOT HARDNESS THROUGH HARDENED BEARING STEEL.

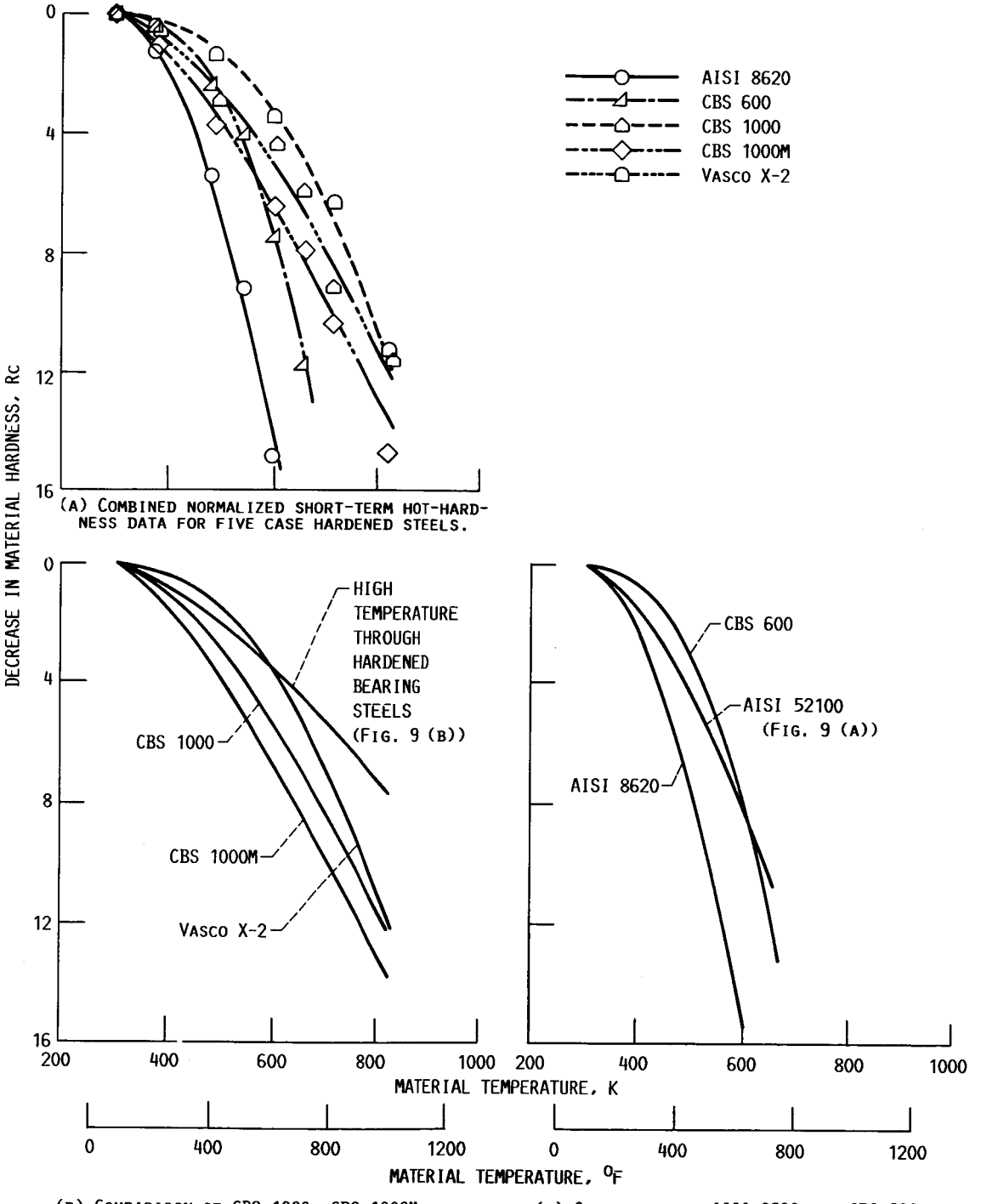

(A) COMBINED NORMALIZED SHORT-TERM HOT-HARDNESS DATA FOR FIVE CASE HARDENED STEELS.

(B) COMPARISON OF CBS 1000, CBS 1000M, AND VASCO X-2 WITH THROUGH-HARDENED HIGH.

(C) COMPARISON OF AISI 8620 AND CBS 600 WITH AISI 52100.

FIGURE 10.- SUMMARY OF CASE HARDENED STEEL SHORT-TERM HOT-HARDNESS DATA AND COMPARISON WITH THROUGH-HARDNESS HIGH-SPEED TOOL STEELS AND AISI 52100.

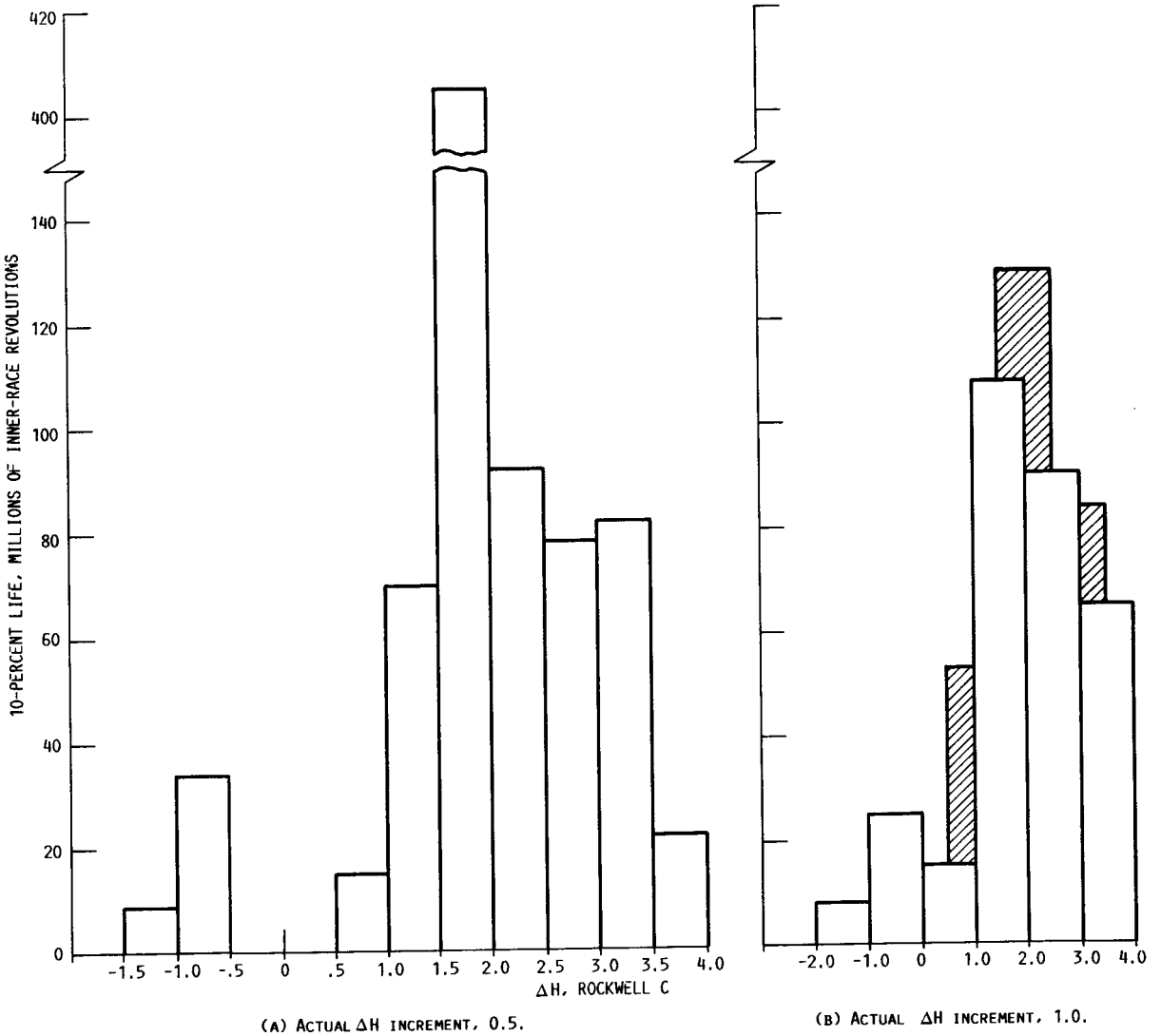

(A) ACTUAL ΔH INCREMENT, 0.5.

(B) ACTUAL ΔH INCREMENT, 1.0.

FIGURE 11.- TEN-PERCENT LIFE AS FUNCTION OF ΔH (DIFFERENCE IN ROCKWELL C HARDNESS BALLS AND RACES) FOR AISI 52100 207-SIZE DEEP-GROOVE BALL BEARINGS.

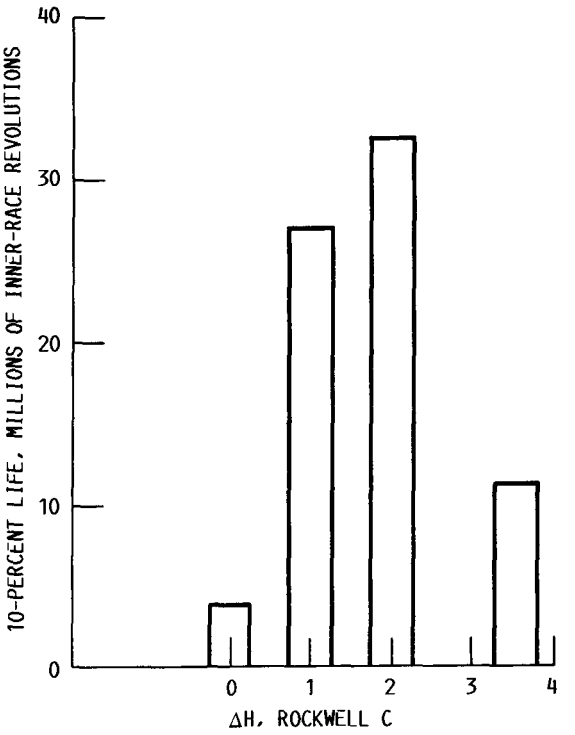

FIGURE 12.- TEN-PERCENT LIFE AS FUNCTION OF ΔH (DIFFERENCE IN ROCKWELL C HARDNESS BETWEEN BALLS AND RACES) FOR AISI 52100 207-S SIZE DEEP-GROOVE BALL BEARINGS.

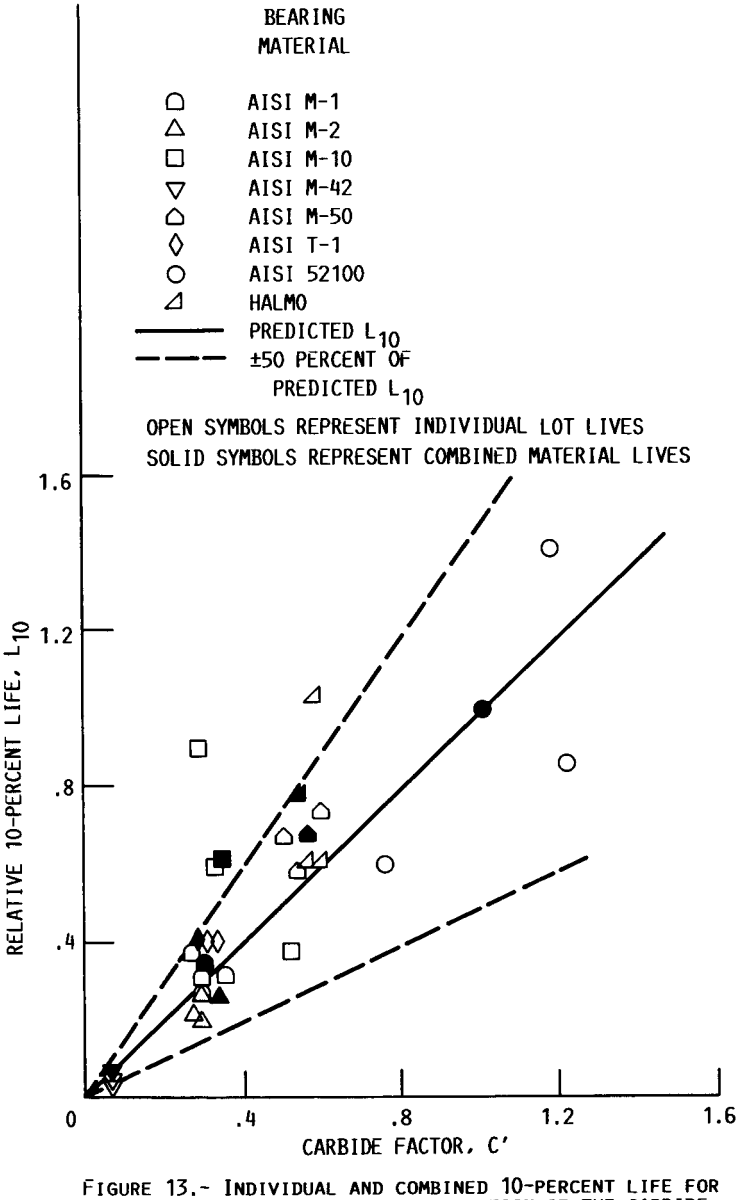

FIGURE 13.- INDIVIDUAL AND COMBINED 10-PERCENT LIFE FOR EIGHT BEARING MATERIALS AS A FUNCTION OF THE CARBIDE FACTOR, C'.

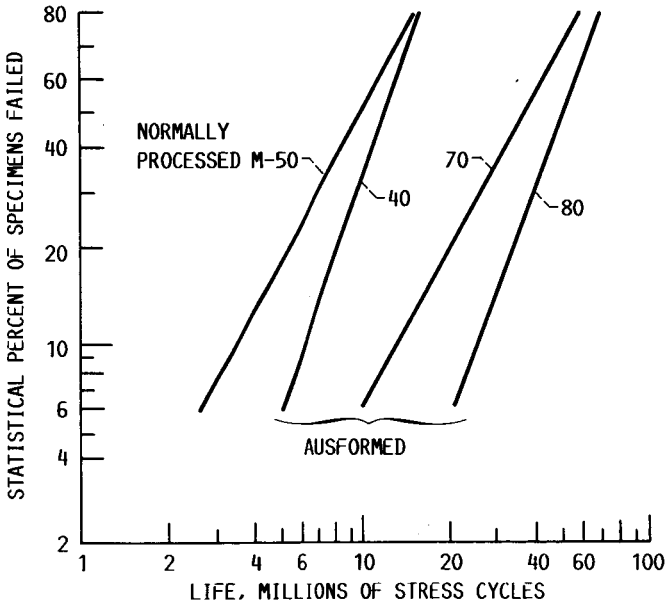

FIGURE 14.- EFFECT OF AUSFORMING ON FATIGUE LIFE FOR AISI M-50 BEARING STEEL.

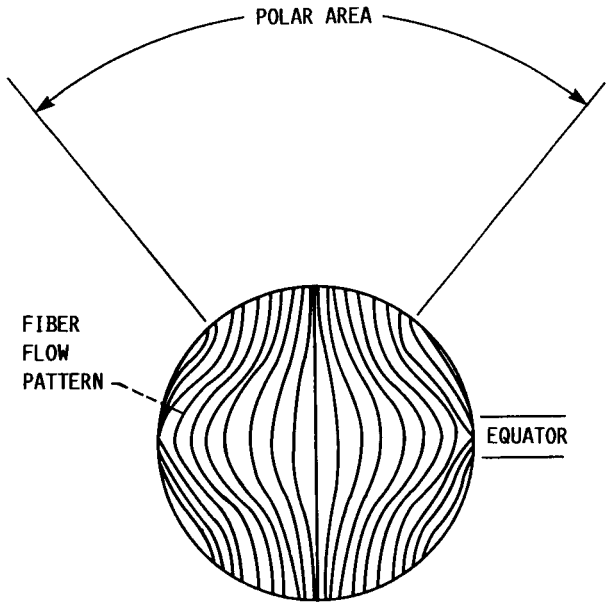

FIGURE 15.- FIBER ORIENTATION IN A BEARING BALL.

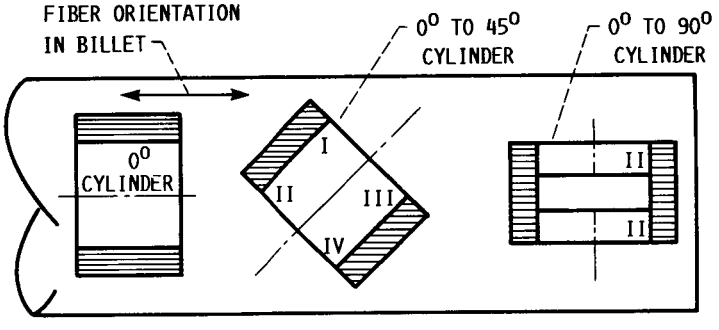

FIGURE 16.- T-1 TOOL STEEL CYLINDER ORIENTATION IN BILLET STOCK.

FIGURE 17. - BEARING RACE SHOWING FIBER FLOW PRIMARILY PERPENDICULAR TO RACEWAY.

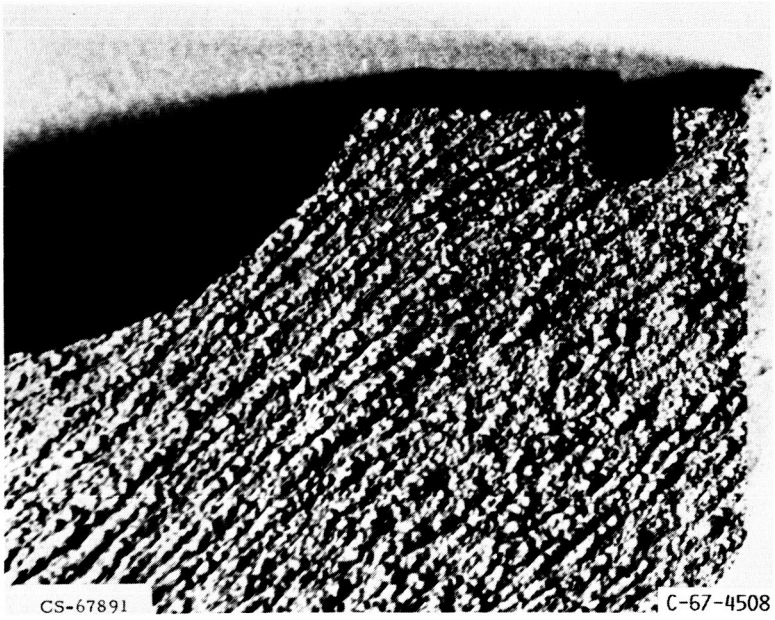

FIGURE 18. - FORGED BEARING RACE SHOWING FIBER FLOW PARALLEL TO RACEWAY.

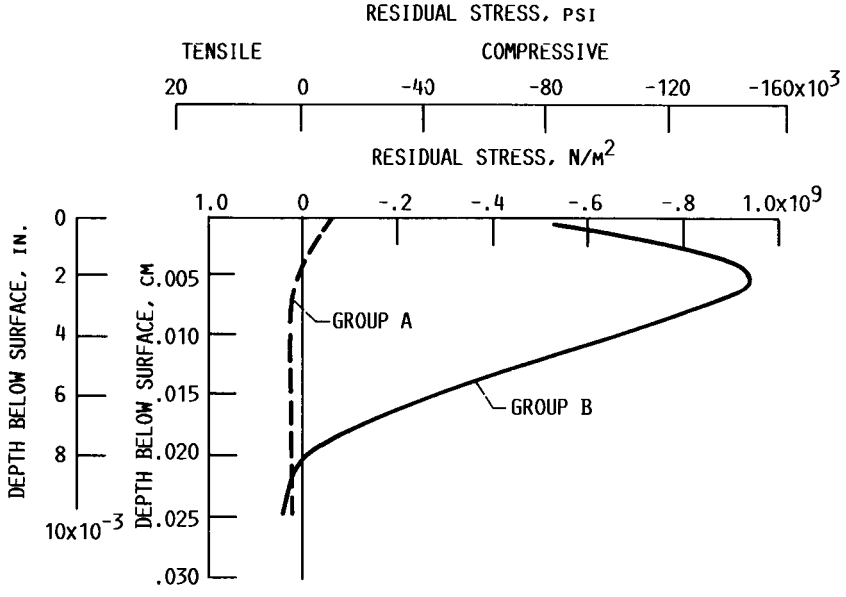

FIGURE 19.- TANGENTIAL RESIDUAL STRESS PATTERNS FOR TWO GROUPS OF 40-MM BORE-SIZE BEARING RACES.

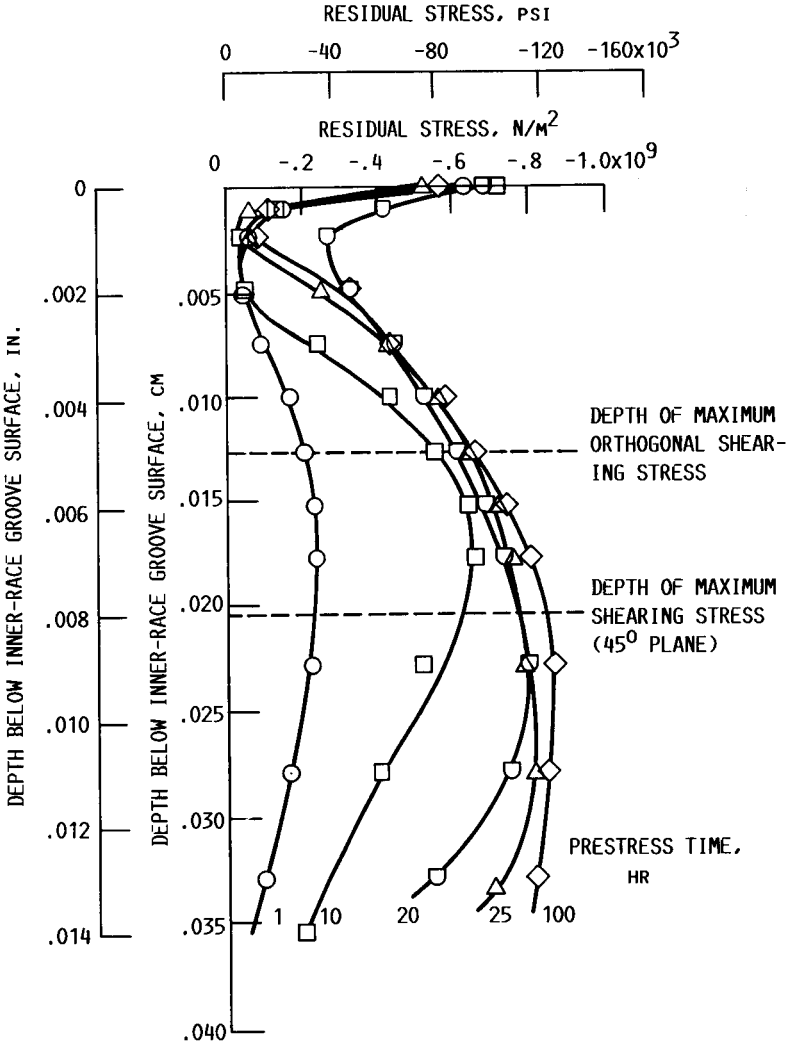

FIGURE 20.- TANGENTIAL RESIDUAL COMPRESSIVE STRESS AS FUNCTION OF DEPTH BELOW CENTER OF INNER-RACE GROOVE FOR VARIOUS PRESTRESS TIME CYCLES FOR 207-SIZE DEEP-GROOVE BALL BEARING. RADIAL LOAD, 13 800 N (3100 LB); MAXIMUM HERTZ STRESS, 3.3×10^9 N/M (480 KSI); SHAFT SPEED, 2750 RPM.

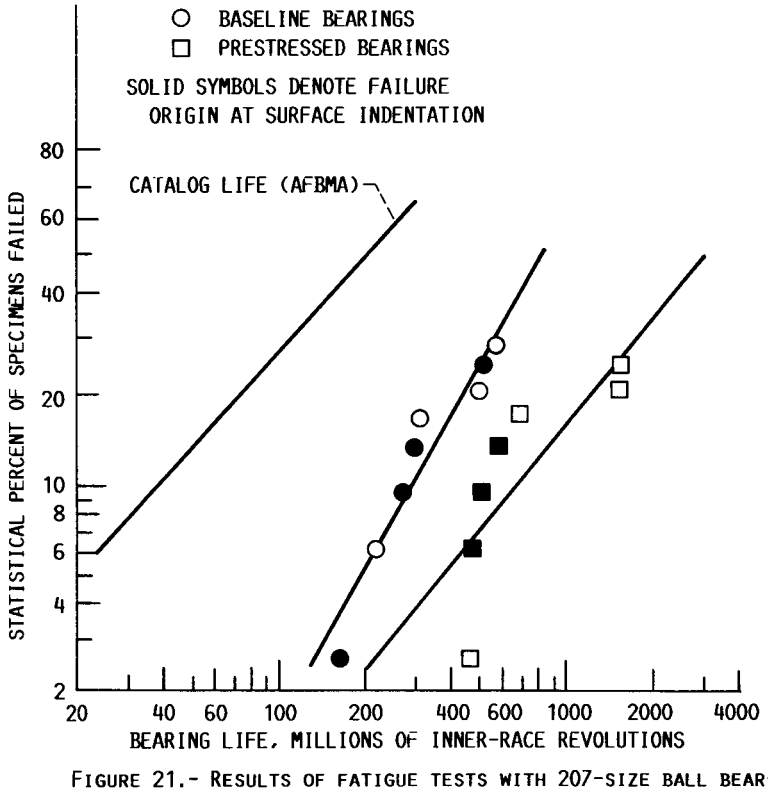

FIGURE 21.- RESULTS OF FATIGUE TESTS WITH 207-SIZE BALL BEARINGS. RADIAL LOAD 5860 N (1320 LB); MAXIMUM HERTZ STRESS, 2.4×10^9 N/M^9 (350 KSI); SHAFT SPEED, 2750 RPM, LUBRICANT, REFINED NAPHTHENIC MINERAL OIL.

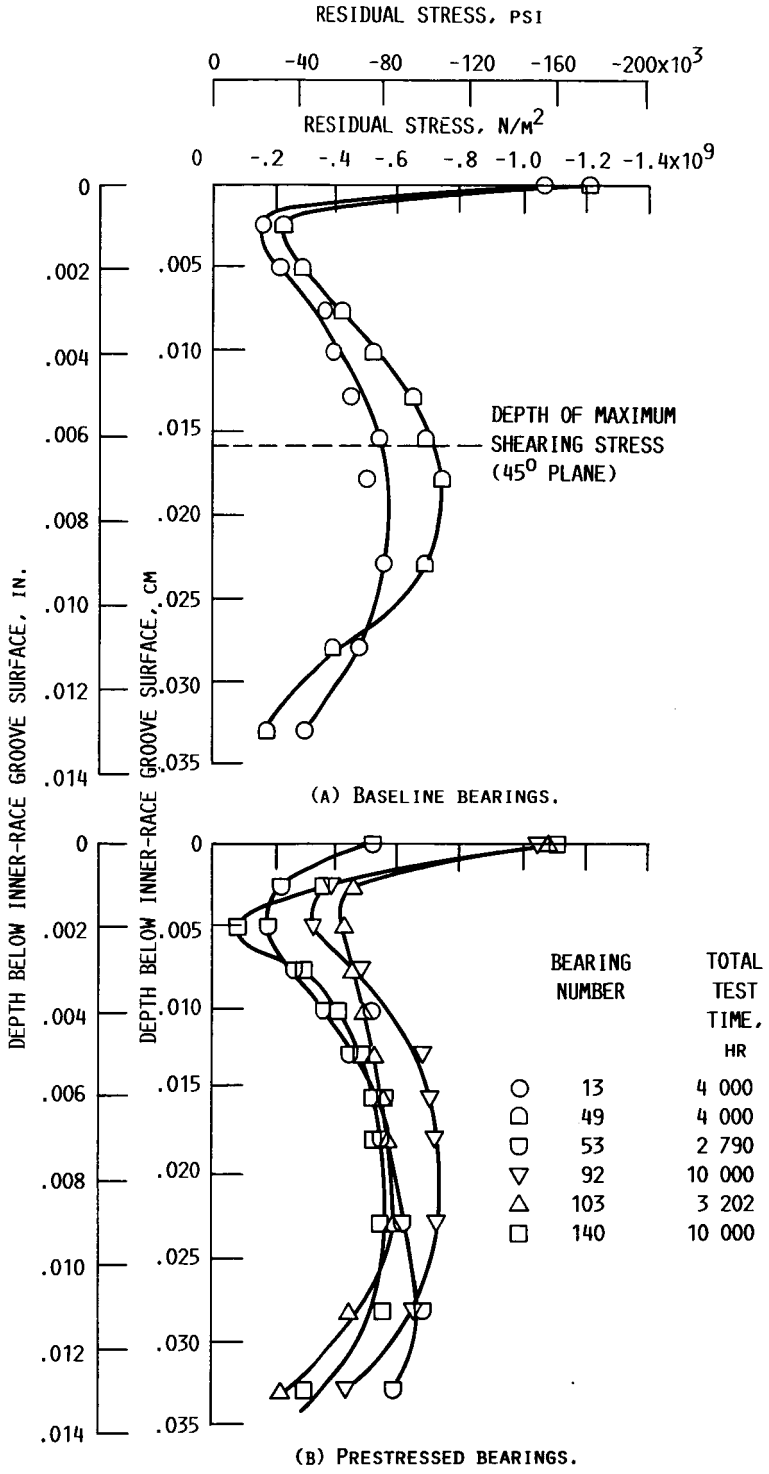

FIGURE 22.- TANGENTIAL RESIDUAL COMPRESSIVE STRESS AS A FUNCTION OF DEPTH BELOW CENTER OF INNER-RACE GROOVE MEASURED AFTER 207-SIZE BALL BEARINGS WERE FATIGUE TESTED. RADIAL LOAD, 5860 N (1320 LB); MAXIMUM HERTZ STRESS, 2.4×10^9 N/M^2 (350 KSI); SHAFT STRESS , 2750 RPM; LUBRICANT, SUPER-REFINED NAPHTHENIC MINERAL OIL.

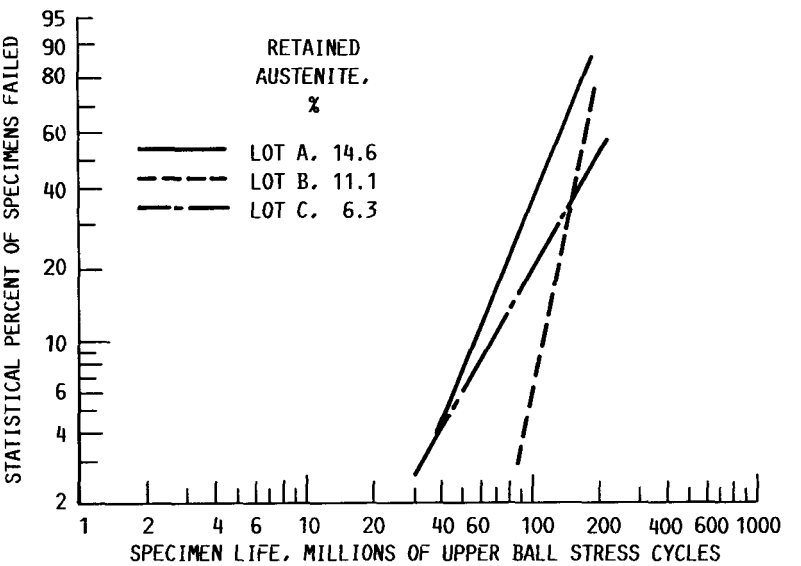

FIGURE 23.- ROLLING-ELEMENT FATIGUE LIVES OF VIM-VAR AMS 5749 HAVING VARIOUS AMOUNTS OF RETAINED AUSTENITE IN FIVE-BALL FATIGUE TESTER. MAXIMUM HERTZ STRESS, $5x52x10^9$ N/m^2 (800 KSI); CONTACT ANGLE, 30^o; SHAFT SPEED, 10 000 RPM; RACE TEMPERATURE, 339 K (150 ^{o}F).

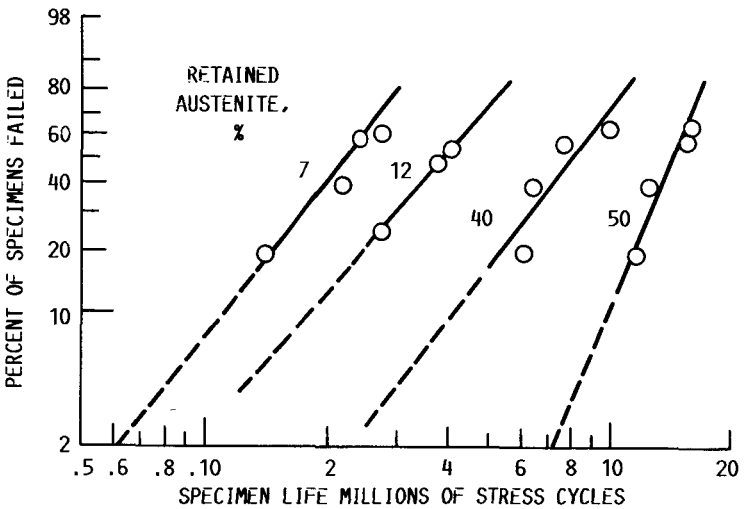

FIGURE 24.- EFFECT OF RETAINED AUSTENITE ON ROLLING-ELEMENT FATIGUE FOR TWO DISKS IN CONTACT. MAXIMUM HERTZ STRESS, 3×10^9 N/M^2 (435 KSI); MATERIAL, 18 CR2NI4WA, SPEED, 2400 RPM FOR DRIVER, 2400 RPM FOR DRIVEN; SLIDING SPEED, 1.05 M/S (41.3 M/S) (SPECIMENS WITH 2 AND 12% RETAINED AUSTENITE WERE TESTED AT MAXIMUM HERTZ STRESS OF 2.8×10^9 N/M^2 (406 KSI)).

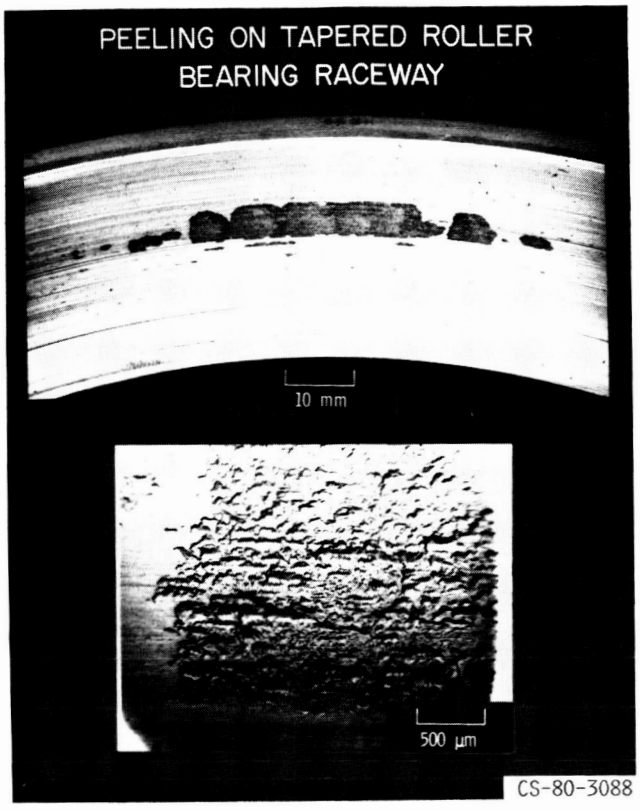

FIGURE 25. - PEELING FAILURE ON CUP RACEWAY SURFACE AFTER 569 HOURS WITH STANDARD DESIGN BEARING RUN AT 12,500 rpm.

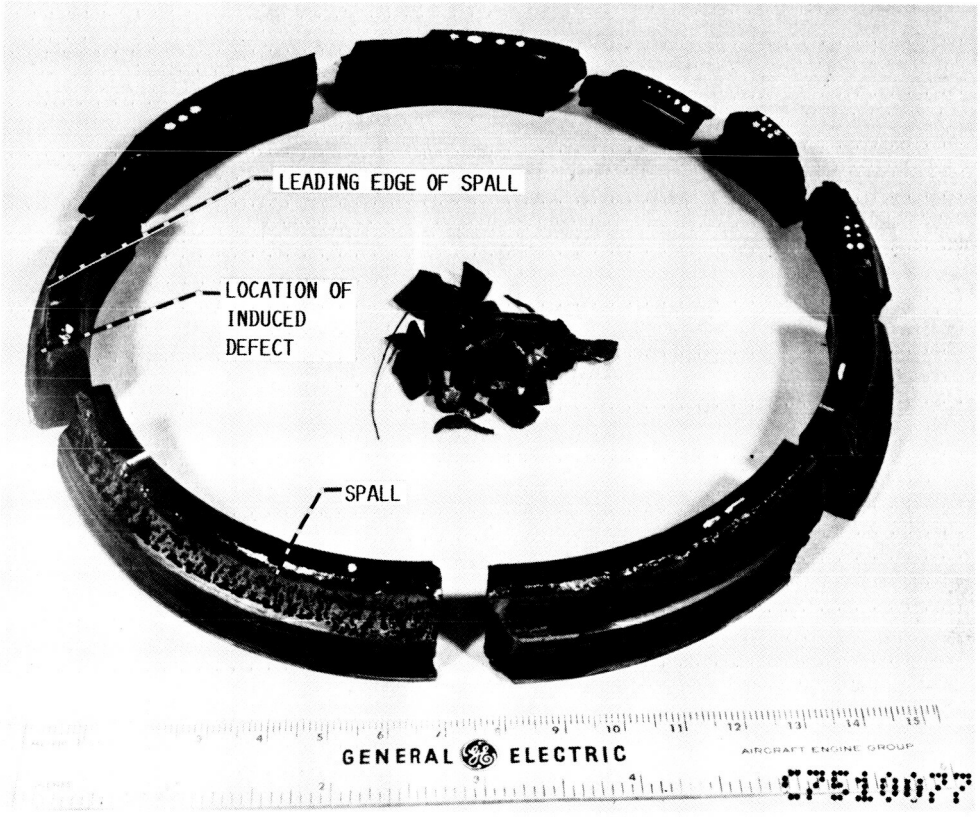

FIGURE 26. - FRACTURED BEARING INNER RACE CAUSED BY INITIATION OF A ROLLING-ELEMENT FATIGUE SPALL.

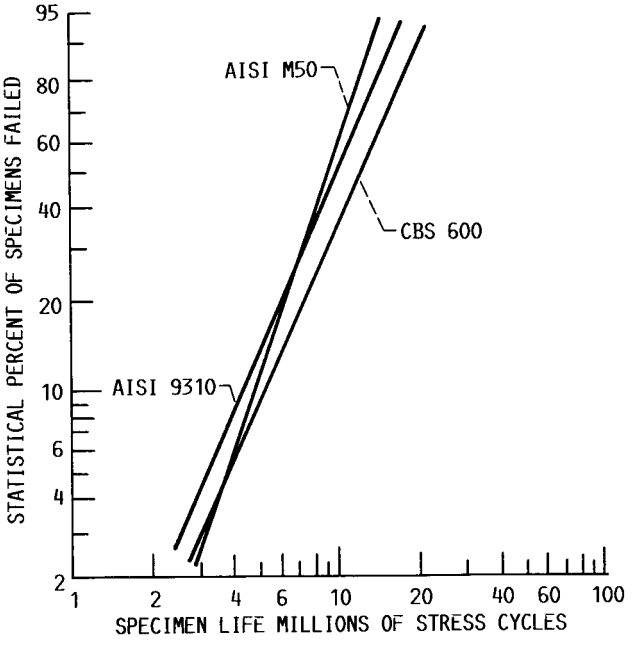

FIGURE 27.- ROLLING-ELEMENT FATIGUE LIVES OF CVM CBS 600, CVM AISI M-50, AND CVM AISI 9310 IN RC FATIGUE TESTER. MAXIMUM HERTZ STRESS, 4.8×10^9 N/M^2 (700 KSI); SPEED, 10 000 RPM; TEMPERATURE, 483 K (74 ^{O}F).

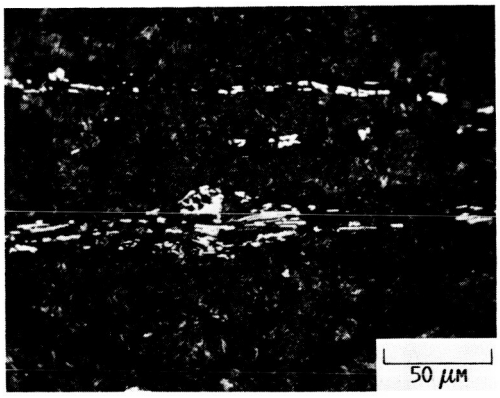

(A) VIM-VAR AISI M-50.

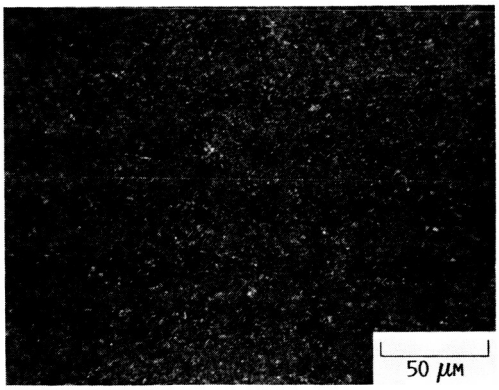

(B) VIM-VAR M-50 NiL.

FIGURE 28. - COMPARISON OF MICROSTRUCTURE OF AISI M-50 NiL. (M-50 NiL HAS SMALLER, MORE UNIFORM CARBIDE STRUCTURE)

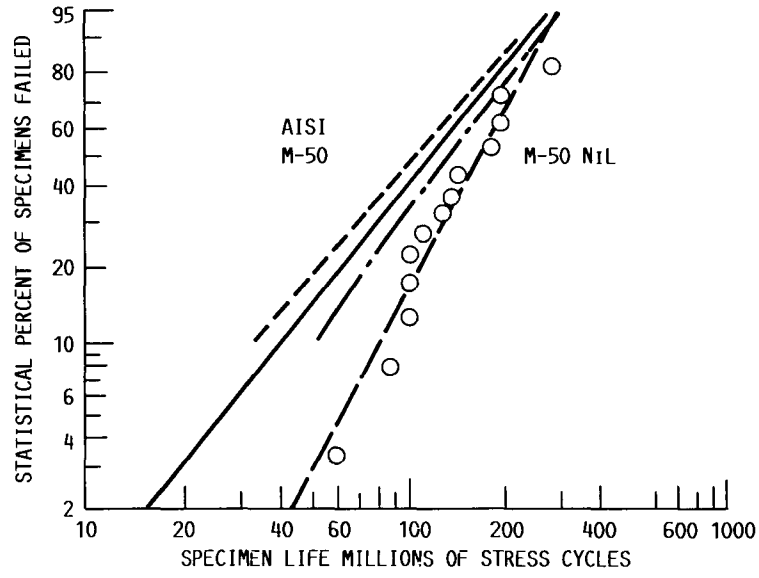

FIGURE 29.- ROLLING-ELEMENT FATIGUE TEST IN RC FATIGUE TESTER OF VIN-VAR AISI M-50 AND CARBURIZED, VIM-VAR M-50 NiL. MAXIMUM HERTZ STRESS, 4.8×10^9 N/m^2 (700 KSI); SPEED, 50 000 RPM; TEMPERATURE, 483 K (74 ^{o}F).

1. Report No.	2. Government Accession No.	3. Recipient's Catalog No.
NASA TM-88881		

4. Title and Subtitle	5. Report Date
Selection of Rolling-Element Bearing Steels for Long-Life Application	6. Performing Organization Code: 505-63-11
7. Author(s): Erwin V. Zaretsky	8. Performing Organization Report No.: E-3288
	10. Work Unit No.
9. Performing Organization Name and Address: National Aeronautics and Space Administration, Lewis Research Center, Cleveland, Ohio 44135	11. Contract or Grant No.
12. Sponsoring Agency Name and Address: National Aeronautics and Space Administration, Washington, D.C. 20546	13. Type of Report and Period Covered: Technical Memorandum
	14. Sponsoring Agency Code

15. Supplementary Notes

Prepared for the International Symposium on the Effect of Steel Manufacturing Processes on the Quality of Bearing Steels, sponsored by the American Society for Testing and Materials, Phoenix, Arizona, November 4-6, 1986.

16. Abstract

Nearly four decades of research in bearing steel metallurgy and processing has resulted in improvements in bearing life by a factor of 100 over that obtained in the early 1940's. For critical applications such as aircraft, these improvements have resulted in longer lived, more reliable commercial aircraft engines. Material factors such as hardness, retained austenite, grain size and carbide size, number, and area can influence rolling-element fatigue life. Bearing steel processing such as double vacuum melting can have a greater effect on bearing life than material chemistry. The selection and specification of a bearing steel is dependent on the integration of all these considerations into the bearing design and application. The paper reviews rolling-element fatigue data and analysis which can enable the engineer or metallurgist to select a rolling-element bearing steel for critical applications where long life is required.

17. Key Words (Suggested by Author(s))	18. Distribution Statement
Bearing materials Rolling-element fatigue	Unclassified - unlimited STAR Category 37

19. Security Classif. (of this report)	20. Security Classif. (of this page)	21. No. of pages	22. Price*
Unclassified	Unclassified		

*For sale by the National Technical Information Service, Springfield, Virginia 22161